People's Democratic Republic of Algeria
Ministry of Higher Education and Scientific Research

University M'Hamed BOUGARA – Boumerdes

Institute of Electrical and Electronic Engineering

Department of Power and Control

Final Year Project Report Presented in Partial Fulfilment of the Requirements for the Degree of the

MASTER

In **Power Engineering**

Option: **Power Engineering**

Title:

Control and Energy Management of Hybrid Electric Vehicles Traction Chain based on BLDC Motor

Presented by:

- **RAHNI Wissem**
- **BOUCHANANE Ikram**

Supervisor:

Dr. AMMAR Abdelkarim

Registration Number:……/2023

Abstract

This work focuses on the development of energy management strategy for hybrid electric vehicles (HEVs) using battery and super-capacitors based on fuzzy logic control . The work is divided into two parts.

In the first part, an energy management strategy is developed for a hybrid energy storage system (HESS) consisting of batteries and super-capacitors. Fuzzy logic is utilized to intelligently distribute and control power, taking into account factors such as state of charge regulation and degradation of on-board energy sources. This approach ensures optimal utilization of available energy under different circumstances .

The second part of the work focuses on motor control in HEVs. Takagi-Suegeno fuzzy logic control is employed to regulate the vehicle's speed, allowing for adaptive and efficient control in various driving conditions.

Simulation tests using MATLAB/Simulink software have been performed in order to validate the proposed techniques. The obtained results will be analyzed and discussed.

By integrating fuzzy logic techniques into energy management and motor control, this work contributes to the development of sustainable and efficient transportation systems. The outcomes aim to reduce emissions, improve fuel efficiency, and promote a greener future for the automotive industry.

Dedication

I would like to dedicate this work to the memory of my grandmother , her love and support have been a force throughout my life, her belief in my abilities have gave me the courage to pursue my academic journey . Your spirit lives on in my heart ,and I am honored to dedicate this work to you. May your soul rest in eternal peace.

To my extraordinary mother, whose unconditional love, sacrifices, and support have provided me with the strength to face any challenge that comes my way, your graceful prayers have accompanied me throughout my entire academic journey. I am forever grateful for your presence in my life.

To my remarkable father, your support, opportunities, and belief in me have been the driving force behind my journey. Your guidance has provided me with the opportunities to continue this path with determination and passion. I dedicate this work to you, expressing my deepest gratitude for the invaluable role you have played in my life.

To my future doctor sister, Sarra, I am truly honored to have you by my side. I dedicate this project to you with profound love and gratitude. Wishing you nothing but the best as you embark on your journey as a doctor.

Lina , to my dear sister who has always been by my side, your support, love, and companionship have been a constant source of strength and comfort throughout my life. You have been there to share both the joys and challenges that life brings.

To my dearest best friend and sister , Aya , your presence in my journey has filled it with cherished memories and unforgettable moments and I am forever grateful for the memories we have created together.

Finally, I want to dedicate this work to my beloved family, especially my aunties who have been a constant source of support from my childhood until now. Your presence in my life has been invaluable, and I am grateful for the love and guidance you have provided me with. I would like also to express my heartfelt appreciation to Uncle Aziz for his motivation, support and encouragement. Your support means the world to me ,and I am truly grateful for your presence. To my dear friends your support and love have touched my heart deeply. This dedication is a heartfelt expression of my deepest appreciation and love for each and every one of you.

Wissem

This work is wholeheartedly dedicated to: Allah, my Creator and my Master, my great teacher and messenger, Mohammed (May Allah bless and grant him).

My lovely parents, whose love, sacrifices, and encouragement have shaped me into the person I am today. Your belief in me and relentless support has been my driving force.

My Beautiful sisters who were always my source joy and delight.

My husband,For your constant love, understanding, and continuous encouragement, always there without hesitation or doubt. Your belief in my abilities has pushed me to strive for excellence.

All my family and my dear friends whoever helped to achieve this work.

Ikram

Acknowledgemnt

In the name of Allah, the Most Merciful and the Most Gracious,

We would like to begin by expressing our gratitude to Allah for His blessings, guidance, and unwavering support throughout this research journey. His mercy and wisdom have been a source of strength and inspiration.

We would also like to extend our heartfelt appreciation to our supervisor, **Dr.Ammar Abdelkarim**, for his invaluable guidance, mentorship, and continuous encouragement. His expertise and wisdom have been instrumental in shaping the direction of this research.

We would like to extend a sincere thank you to **Mr. Oubelaid Adel** for his valuable support and contributions throughout this research.

We would like to acknowledge and appreciate the teachers and staff of **The Institute of Electrical and Electronics Engineering** for their knowledge, guidance, and support throughout our academic journey. Their dedication and expertise have greatly contributed to our growth and learning.

Lastly, We would like to express our sincere gratitude to our family, friends, and loved ones for their unwavering belief in us, their love, and their constant support. Their encouragement and presence have been a source of motivation and strength.

Contents

List of Figures

List of Tables

List of Abbreviations

HEV: Hybrid Electric Vehicle

HESS: Hybrid Energy Storage System

IC: Internal Combustion Engine

EM: Electric Motor

ESS : Energy Storage System

DC : Direct Current

AC : Alternating Current

EV : Electric Vehicle

BAS : Belt Alternator Starter

MHEV : Mild Hybrid Electric Vehicle

PHEV : Plug-in Hybrid Electric Vehicle

SC : Supercapacitor

PV : Photovoltaic

Ni-Cd : Nickel-Cadmium

Ni-MH : Nickel-Metal Hydride

Li-ion : Lithium-ion

EDLC : Electric Double Layer Capacitor

PC : Pseudo-Capacitor

HSC : Hybrid Supercapacitor

RTIL : Room Temperature Ionic Liquid

SSP : Solid State Polymer

ESR : Equivalent Series Resistance

BLDC : Brushless DC (Electric) Motor

PMSM : Permanent Magnet Synchronous Motor

BU : Battery Unit

PI : Proportional-Integral

MOSFET : Metal-Oxide-Semiconductor Field-Effect Transistor

EMF : Electromotive Force

ECE cycle : Economic Commission for Europe cycle

NEDC : New European Driving Cycle

FTP-75 : Federal Test Procedure-75

EMS : Engine Management System

RB : Regenerative Braking

OB : On-Board

SOC : State of Charge

GA : Genetic Algorithm

FLC : Fuzzy Logic Controller

TS-FLC : Takagi-Sugeno Fuzzy Logic Control

MILP : Mixed Integer Linear Programming

PSO : Particle Swarm Optimization

SA : Simulated Annealing

PWM : Pulse Width Modulation

General Introduction

The transportation sector is responsible for a significant portion of global carbon dioxide emissions, which contribute to climate change. To address this issue, researchers and policymakers have been exploring alternative energy sources for vehicles. Electric vehicles, including hybrid electric vehicles (HEVs), have emerged as a promising solution. One of the critical aspects in the development of HEVs is effective energy management, which involves optimizing the utilization of different energy sources and controlling the power flow within the vehicle system.

The energy management of HEVs plays an essential role in maximizing fuel efficiency and minimizing environmental impact. It encompasses various aspects, including the selection and integration of different energy storage technologies, control strategies for power allocation, and management of energy flows during different driving conditions. Efficient energy management ensures the optimal utilization of energy sources, such as batteries and super-capacitors, while considering factors like driving cycles, power demands, and system constraints.

The main objective of this work is to delve into the energy management of hybrid electric vehicles using battery and super-capacitor technologies. We explore the application of fuzzy logic control techniques to enhance the performance and efficiency of both the traction chain and the hybrid energy storage system (HESS). The report is divided into several chapters, each focusing on specific aspects of energy management and control.

Chapter 1:

The first chapter provides a comprehensive overview of the history of electric vehicles, hybrid electric vehicles, and the evolution of HEV architectures. We also explore different storage technologies, including batteries and super-capacitors, and examine various types of electric motors commonly used in HEVs. Additionally, we discuss driving cycles and

their impact on energy management.

Chapter 2:

Chapter 2 focuses on the proposed topology and mathematical models associated with the hybrid energy system (HES) and the brush-less DC (BLDC) motor. The chapter begins by introducing the proposed topology for the HES, which includes components such as the battery, super-capacitor, DC-DC converter, and inverter. This topology is designed to optimize the energy management and utilization of the HES in the hybrid electric vehicle.

Chapter 3:

The third chapter delves into the control of the traction chain in HEVs. It is divided into two parts, starting by the control of the hybrid energy storage system with DC/DC converters. The second part focuses on the control strategies for BLDC motors using Takagi-Suegeno fuzzy logic controller. The fuzzy logic approach have been used as energy management algorithm to ensure optimal utilization of the battery and super-capacitors under pre-defined driving cycles.

Chapter 4:

Through the simulation results and discussions, the fourth chapter presents the performance evaluation of the system through different scenarios, including constant speed with load variation, acceleration and deceleration with hybrid energy storage, and the Japanese driving cycle. These scenarios are simulated using MATLAB/Simulink, and the results are analyzed and discussed in details.

Chapter 1

Overview about Hybrid Electric Vehicles

1.1 Introduction

There are several types of HEVs available, including parallel hybrids, series hybrids, and plug-in hybrids. Parallel hybrids use both the engine and electric motor to power the wheels simultaneously, while series hybrids use the engine to generate electricity to power the motor. Plug-in hybrids can be charged using an external power source, allowing them to operate in electric-only mode for a certain distance before switching to gasoline power.

In recent years, there have been several advancements in HEV technology, including improvements in storage systems(i.e. batteries, super-capacitors and fuel cell), as well as the development of more efficient and powerful electric motors(i.e. PMSMs,BLDCs...). As a result, HEVs are becoming more attractive to consumers and are expected to play an increasingly important role in reducing emissions from the transportation sector. In this chapter an overview about HEVs, their technologies and types of electrics motors will be presented.

1.2 History of electric vehicles

The combination of batteries and electric motors powering the wheels of light vehicles can be traced back to the 1830s with the emergence of the first non-rechargeable battery-powered electric vehicles [1].

The rechargeable lead-acid battery was invented by Gaston Planté in 1859 and remains widely used for energy storage today. Alphonse Camille Faure further improved the capacity of these batteries, leading to large-scale production and the proliferation of autonomous electric vehicles on city streets in 1881. Electric cars entered the commercial market in the late 20Th century, thanks to the development of rechargeable batteries [2]. Therefore, it can be said that the dominance of electrical energy accumulation and its conversion to mechanical energy has made it possible for a new, quiet, and clean method of urban mobility.

In 1837, Robert Davison Aberdeen created the first electric carriage in England, powered by an iron-zinc battery and an electric motor. Charles Jeantaud Raffard conducted experiments in France, and Werner Siemens improved the electric motor in Germany. Despite steam-powered vehicles dominating at that time, electric vehicles emerged as the preferred choice for urban traffic due to their quiet operation and environmentally friendly drive system [3].

1.3 Hybrid Electric Vehicles

A hybrid electric vehicle combines a conventional internal combustion engine (ICE) propulsion system with an electric propulsion system. These propulsion systems can be combined in various ways to accomplish different objectives. The presence of the electric power-train is designed to realize better fuel economy than a conventional vehicle or better performance. Another type of HEVs uses only electric propulsion system with hybrid power source that combines batteries with another secondary energy source such as super-capacitors, fuel cell or PV panel.

The most common practice as an HEV energy storage device is using an electrochemical battery and super-capacitors.

The control strategy of an HEV can be designed for various purposes, based on the different combinations of power flows and, in order to satisfy load requirements, the HEV can select any power flow path. This liberty to select various power flow combinations creates much more flexibility of operation than the conventional vehicles. Moreover, in an HEV drive-train, vehicle braking energy can also be recuperated efficiently [4].

Based on different combinations of electric and mechanical traction, HEV drive-trains are divided into three basic architectures: series, parallel, and series parallel hybrids [5]. The specific choice of a HEV configuration depends on several factors including the type of the application, cost and weight considerations and expectations of the targeted customers.

1.4 The hybrid electric vehicle technologies

HEV (Hybrid Electric Vehicle) technologies refer to the different types of vehicles that combine two or more power sources, such as an internal combustion engine (ICE) and an electric motor, to improve the overall performance and efficiency of the vehicle. These technologies are gaining popularity due to their ability to reduce fuel consumption and emissions while providing a better driving experience.

1.4.1 Full hybrid

Full hybrids maximize hybridization by combining electrical power and combustion engine power for vehicle propulsion. They can operate in electric mode, engine mode, or a combination of both. However, they still rely on petrol as their energy source, resulting in some level of pollution, noise, and vibration from the combustion engine.

Toyota's hybrid electric vehicle system includes an internal combustion engine, a power control unit, motor generators for propulsion and energy regeneration, a high voltage battery, and a power split device. Full hybrids typically have both high voltage and low voltage electrical systems, with a low voltage battery and a DC to DC converter to power the low voltage system.

Full hybrids offer increased vehicle efficiency without the need for external battery charging [6].

1.4.2 Mild hybrid

Mild hybrids, also known as MHEVs, have limited electric power contribution compared to other hybrid systems. They rely on the internal combustion engine as the main power source, with the electric motor providing assistance rather than sole propulsion. This

electrical assist helps improve efficiency through features like quick start-stop functionality, torque boost, and regenerative braking. The battery in MHEVs is recharged through engine rotation and regenerative braking, eliminating the need for external charging. However, emissions, vibrations, and noise are still present in this type of hybrid configuration [7].

MHEV Essential Components

A typical mild hybrid vehicle includes an internal combustion engine (ICE), a belt alternator starter (BAS) with an inverter, a 48-Volt battery, a 12-Volt battery, and a DC to DC converter. The IC engine generates mechanical torque through combustion to propel the vehicle. The BAS combines the functions of a starter and an alternator, enabling energy recuperation during braking and providing a quick start-stop system. The 48V battery stores energy generated by the BAS and powers the 48V system. A DC to DC converter converts the 48V electricity to 12V for storage in the 12V battery, which powers the entire 12V electrical system of the vehicle.

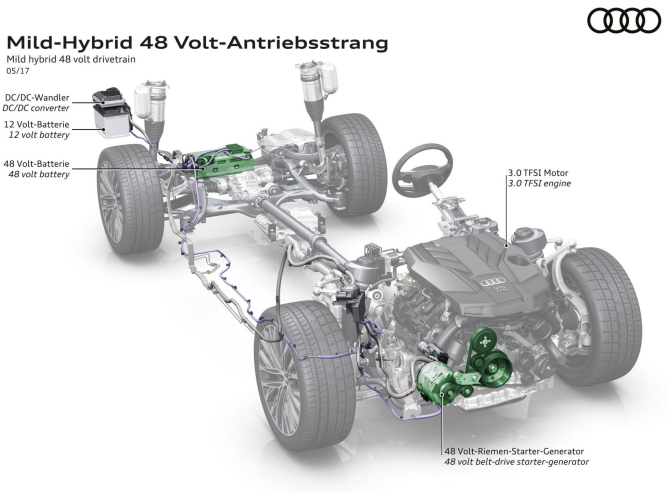

Figure 1.1: Mild hybrid 48 V Antribsstrang

1.4.3 Plug-in hybrid

A plug-in hybrid vehicle is an HEV with the ability to recharge its energy storage system with electricity from the electric utility grid. The PHEVs have a battery pack (or ESS) of high energy density that can be externally charged by connecting a plug to an external electric power source, and can run only with electric power for more time than regular

HEVs [8]. The conversion of HEVs to PHEVs involves adding or replacing the ESS to improve efficiency and increase the electric range. The ESS, consisting of a battery pack, stores energy from external charging and regenerative braking for the traction motor system. Recharging is done through an AC outlet charger with an AC-DC converter and digital controller. A bidirectional DC-DC converter and charge-discharge profile enable energy transfer between the ESS and the motor system [9].

Benefits and Obstacles of PHEVs

PHEVs offer the advantage of utilizing multiple energy sources, reducing petroleum consumption and dependence on fossil fuels. They provide benefits in both electric and liquid fuel modes. However, PHEV technology also comes with limitations and challenges that need to be taken into consideration [10].The principal technical obstale concerns the ESS cost, volume, and life that must be studied very well to be really usable. More stored energy means more miles that the vehicle can be driven electrically. However, increasing the ESS also increases vehicle cost and means a bigger size of the pack [11].

1.5 Different storage technologies

Storage technologies refer to the methods and devices used for storing energy. In the context of electric vehicles, energy storage is essential for providing power to the electric motor that drives the vehicle. The two most common storage technologies used in electric vehicles are batteries and super-capacitors.

1.5.1 Batteries

A battery is a device that converts chemical energy into electrical energy through an electrochemical reaction. It comprises one or more electrochemical cells, each consisting of a positive electrode (cathode), a negative electrode (anode), and an electrolyte. When a battery is connected to an external circuit, electrons flow from the negative electrode through the circuit to the positive electrode, generating an electric current. In recent years, the development of batteries has made great progress. Furthermore, the global production of electric vehicle batteries has increased by 66% [12].which is undoubtedly directly related to the increase in vehicle sales, and forecasts show that the demand for

batteries will continue to grow. In fact, it is predicted that the supply and demand for electric vehicles will only increase in the coming years. There are different battery technologies [13] :

- Lead-acid batteries: Lead-acid batteries are the oldest type of rechargeable batteries. They are widely used in automotive applications and as backup power supplies due to their robustness and relatively low cost.

- Nickel-cadmium batteries (NiCd): NiCd batteries have been widely used in portable electronics and power tools. They offer good performance at low temperatures and have a long cycle life.

- Nickel-Metal Hydride batteries (NiMH): NiMH batteries are commonly used as a replacement for NiCd batteries. They have a higher energy density, making them suitable for portable electronics and hybrid vehicles.

- Lithium-ion batteries (Li-ion): Li-ion batteries have become the most popular rechargeable battery technology. They offer high energy density, low self-discharge rates, and long cycle life. Li-ion batteries are used in a wide range of applications, including smartphones, laptops, electric vehicles, and renewable energy systems.

Each type of battery has its own advantages and limitations, and the choice of battery depends on the specific requirements of the application, such as energy density, cycle life, cost, and environmental impact.

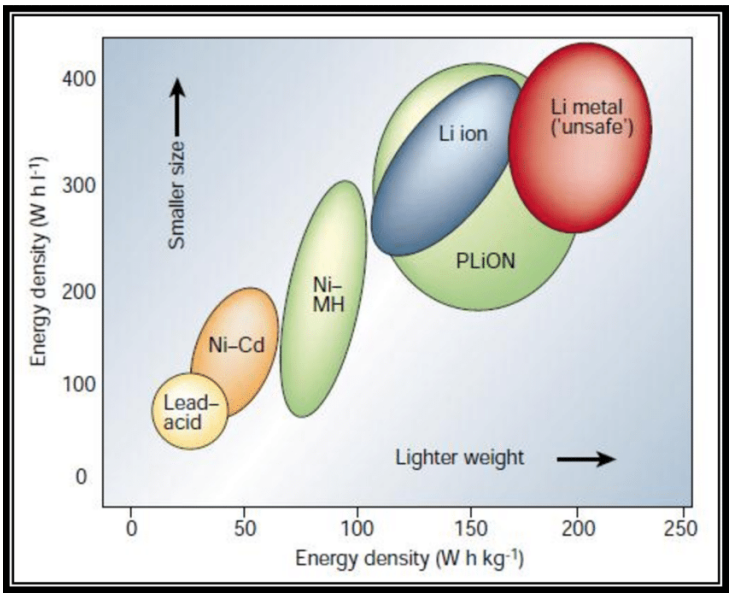

Figure 1.2: Comparison of the different battery technologies in terms of volumetric and gravimetric energy density

In this study, lithium-ion batteries will be used due to their superior energy densities compared to nickel-metal hydride or lead-acid batteries. Figure 1.3 illustrates the operating principle of a lithium-ion battery. During the discharge process in a lithium-ion battery, a series of chemical reactions occur. In the lithium-graphite anode, lithium ions (Li) are oxidized from the 0 oxidation state (Li) to +1 oxidation state (Li+). This oxidation reaction is represented by the following equation [14]:

$C_6Li_2^- \longrightarrow 6\,C(\text{graphite}) + Li^+ + e^-$

The lithium ions produced during the anode reaction then migrate through the electrolyte medium to the cathode. In the cathode, lithium ions are incorporated into lithium cobalt oxide ($LiCOC_2$) through a reduction reaction. This reduction reaction involves the reduction of cobalt from a +4 oxidation state to a +3 oxidation state. The equation for this reaction can be expressed as follows [14]:

$Li_{1-x}CoC_2(s) + xLi^+ + xe^- \longrightarrow LiCoC_2(s)$

It is important to note that these reactions can be reversed during the battery's charging process. In this case, the lithium ions leave the lithium cobalt oxide cathode and migrate back to the anode. At the anode, they are reduced back to neutral lithium and reincorporated into the graphite network, preparing the battery for subsequent discharge cycles.

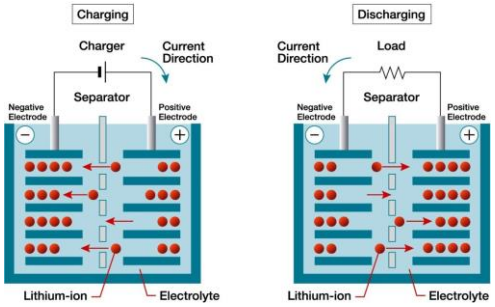

Figure 1.3: Operating principle of a lithium-ion battery.

1.5.2 Supercapacitors

In recent years, there has been a growing interest in Supercapacitors (SCs) as an alternative energy storage technology that complements rechargeable batteries. SC technology has evolved and shown potential for commercial-scale energy storage. Compared to traditional rechargeable batteries, SCs have short charge/discharge times, a long cycle life, are lightweight, and environmentally friendly. Table 1.1 compares the characteristics of rechargeable batteries (such as lithium-ion) and SCs.

As seen in Table 1.1, electrochemical batteries have high energy densities, typically ranging from 70-100 (Wh/kg) for commercially available systems. They can store a large amount of energy that can be released over a longer period of time. In contrast, SCs have a lower energy density, with a commercially used cell typically ranging from 0.5-30 Wh/kg, but can be released in an exceptionally short discharge period. Table 1.1 also provides useful information on other distinct characteristics of SCs that make them complementary devices alongside rechargeable batteries. However, addressing inherent weaknesses in technical performance characteristics of SCs requires immense research efforts to make them commercially successful [15].

Characteristics	Super-capacitors	Lithium-ion batteries
Cycle life	500,000	800-3000
Power density (kW/kg)	13	0.5-1
Energy density (Wh/kg)	0.5-30	70-100
Cycle efficiency (%)	98	Up to 95
Charge/discharge time	0.3-30 s	0.3-3h
Capital cost ($/kWh)	300-2000	600-2500
Durability (years)	20	14-16

Table 1.1: Performance characteristics comparison of supercapacitors and rechargeable batteries (lithium-ion).

Development of supercapacitor's (SCs) technology

Super-capacitors are also known as ultra-capacitors or electrochemical capacitors. They store charge through the separation of ionic and electronic charges at the electrode/electrolyte interface, forming an electric double layer. This double layer is very thin and has a high specific surface area, enabling super-capacitors to have very high specific capacitances and superior energy densities compared to conventional electrostatic capacitors [16].

Super-capacitors, particularly electric double layer capacitors (EDLCs), offer a nearly limitless cycle life due to their interfacial surface charge storage mechanism without chemical or phase changes in the active materials. Super-capacitors offer high capacity retention, up to 99%, and are known for their safety and environmental friendliness. They have a simpler design compared to rechargeable batteries, using fewer electrolytes and facilitating easy operation and recycling. The performance of supercapacitors is influenced by the choice of electrolytes, which affects breakdown potentials, operating voltages, and energy densities. The viscosity of electrolyte solutions also impacts power densities. Supercapacitor cells can be assembled in two electrode or three electrode configurations, with the latter providing higher measurement accuracy. Schematic representations of both configurations are shown in Figure 1.4 .

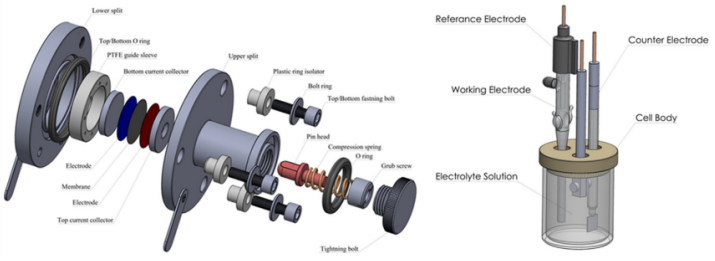

Figure 1.4: Graphical representation of two and three electrode cells (a) two electrode configuration (b) three electrode configuration

Classification of super-capacitors

Super-capacitors can be classified into three main categories based on their assembly, charge storage mechanism, and electrode/electrolyte materials. Since each configuration has a distinct charge storage mechanism, they exhibit unique signature characteristics that define each type, including EDLC, PCs, and HSCs [17].

1. Electric double layer capacitors (EDLCs)

EDLCs, or electric double-layer capacitors, are widely used and commercially available super-capacitors that rely on physical adsorption of electrolyte ions on the surface of highly porous carbon electrodes. Activated carbon is the most commonly used electrode material in commercial EDLCs. While researchers are exploring synthetic carbons like graphene and carbon nanotubes in the laboratory, their high production costs and complex synthesis procedures limit their commercial viability. New electrolytes, such as room temperature ionic liquids (RTILs) and solid-state polymer (SSP) electrolytes, are being investigated, but their higher viscosities and lower ionic conductivities pose challenges for widespread adoption.

2. Pseudo-capacitors (PCs)

   Pseudocapacitors (PCs) offer better capacitor performance and higher energy densities compared to EDLCs, but lower energy densities compared to rechargeable batteries. PCs rely on reversible redox reactions for charge storage, resulting in fast and fully reversible electronic transfer. However, PCs suffer from lower power densities due to their higher equivalent series resistance (ESR), except for costly materials like ruthenium oxide. PCs are still in the early stages of commercialization, with various transition metal oxides and conducting polymers being explored as electrode materials. Promising materials include manganese oxide, iron oxide, cobalt oxide, nickel oxide, and derivatives of polythiophene, polypyrrole, and polyaniline. Further research is needed to make these materials commercially viable.

3. Hybrid super-capacitors (HSCs)

Hybrid super-capacitors (HSCs) can be configured in various ways, combining capacitive and battery-type electrodes in symmetric and asymmetric configurations. They exhibit electrochemical behavior between that of batteries and capacitors, utilizing high working potentials to initiate reversible redox reactions and complement double-layer energy storage. HSCs show increased capacitive behavior but suffer from lower power densities, poor cyclic life, and sluggish kinetics. To address these issues, researchers are exploring new nanostructure materials and conductive additives like graphene and carbon nanotubes. Different types of super-capacitors use various electrolyte solutions, including aqueous and non-aqueous solutions such as organic solutions and ionic liquids.

1.6 Different type of electric motors used for HEV

The main component of an electric vehicle that transforms electrical energy from the battery into rotational motion is the electric motor. The electric motor is responsible for converting electrical energy into mechanical energy, which is then used to propel the vehicle. It operates based on the principles of electromagnetism, utilizing the interaction between magnetic fields and electric currents to generate rotational force. The electric motor plays a crucial role in the overall performance and efficiency of an electric vehicle, as it determines the power, torque, and speed characteristics of the vehicle's propulsion system. Various types of electric motors can be used in electric vehicles, including brushed DC motors, brush-less DC motors, and induction motors, each with its own advantages and considerations.

1.6.1 Most used motor types in HEVs

Electric vehicles (HEVs) utilize different types of motors for their propulsion. In this project, the focus will be on investigating the Brush-less DC (BLDC) motor. Table 1.2 provides a comprehensive Comparison of different types of motors which are extensively used in EV application [18].

Features	Brush-less DC Motor	Induction Motor(IM)	Brushed DC Motor (BDM)	Permanent Magnet Synchronous Motor (PMSM)
Efficiency	High	Low	Moderate	High
Maintenance	Very low	Low	Periodic	Lower
Switching Losses	Less	High	High	High
Speed Range	High	Low	Moderate	Higher
Electrical Noise	Low	Low	Noisy	Low
Speed/Torque characteristic	Highly	Flat	Non-linear	High
Cost	High	Low	Low	Higher

Table 1.2: Comparison of Motors for EV Application

1.7 Hybrid energy storage system HESS

The Energy Storage System (ESS) in EVs and HEVs consists of batteries and ultra-capacitors. Batteries have high energy but low power, while ultra-capacitors have high

power and capacity. Hybrid Energy Storage Systems (HESS) combine multiple storage units, and innovative designs are being developed. The Ragone curve, shown in Fig. 1.5 , demonstrates the specific energy of fuel cells, batteries, ultra-capacitors, and conventional capacitors, versus their corresponding specific power levels . As depicted in this figure, batteries with high specific energy and low specific power are placed more towards top left of the figure while ultra-capacitors approach the opposite corner due to their high specific power and low specific energy [19].

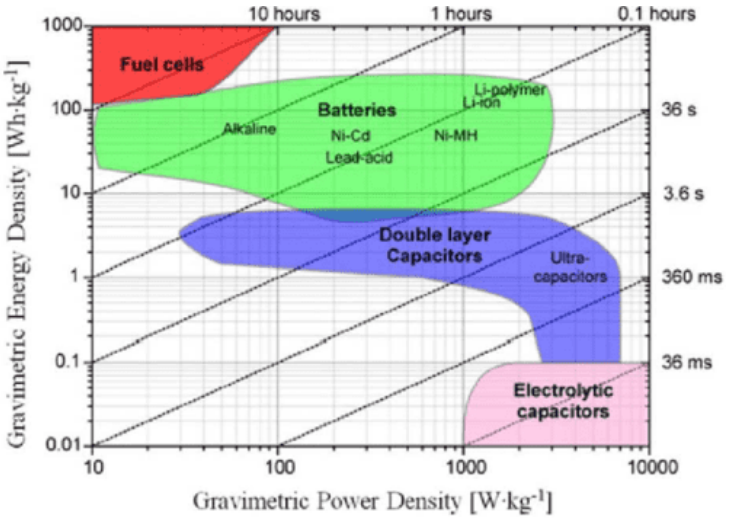

Figure 1.5: Specific energy versus specific power for various ESSs

Interfacing battery unit and super-capacitors unit to the DC bus in a drive-train

One of the primary obstacles in configuring a Hybrid Energy Storage System (HESS) is how to connect the battery and ultra-capacitor units to the DC bus. Figure 1.6 provides a detailed illustration of different HESS topologies, each with its own advantages and disadvantages. The following subsections will provide a brief overview of these topologies.

- **Direct connection of BU and SC to the DC bus**

The direct connection of BU and SC to the DC bus, as shown in Figure 1.6 (a), represents the simplest way of interfacing battery and super-capacitor units [20].

- **Partially-decoupled configurations**

Partially-decoupled Hybrid Energy Storage System (HESS) configurations involve the use of a DC-DC converter to decouple either the Battery Unit (BU) or Super-capacitor (SC)

from the DC bus. This configuration adds to the system cost and control complexity but offers important features. There are two topologies: Topology I Fig 1.6 (b), where the SC is directly connected to the DC bus, and Topology II, where the BU is directly connected to the DC bus while the UC is interfaced to the bus via the DC-DC converter [21].

- **Fully-decoupled configurations**

Fully-decoupled HESS configurations use a power electronic system to completely isolate the BU and SC from the DC bus. By implementing a power management algorithm, the system can control the operation of both units and improve overall performance, leading to a longer life for the BU. However, this type of configuration is typically more expensive due to the complex power electronic structure and control circuitry involved. The system may also experience higher losses due to the use of numerous semiconductor devices and passive elements. There are several topologies within the fully-decoupled category, including the simplest configuration in Fig. 1.6 (d) where a DC-DC converter decouples parallel-connected BU and SC from the DC bus. More complex cascaded topologies are shown in Figs. 1.6 (e) and (f), where two cascaded converters are used to decouple BU and SC from the DC bus.Fig. 1.6 (g) depicts the parallel-converter topology, which is a widely adopted and favorable fully-decoupled configuration in this category [22].

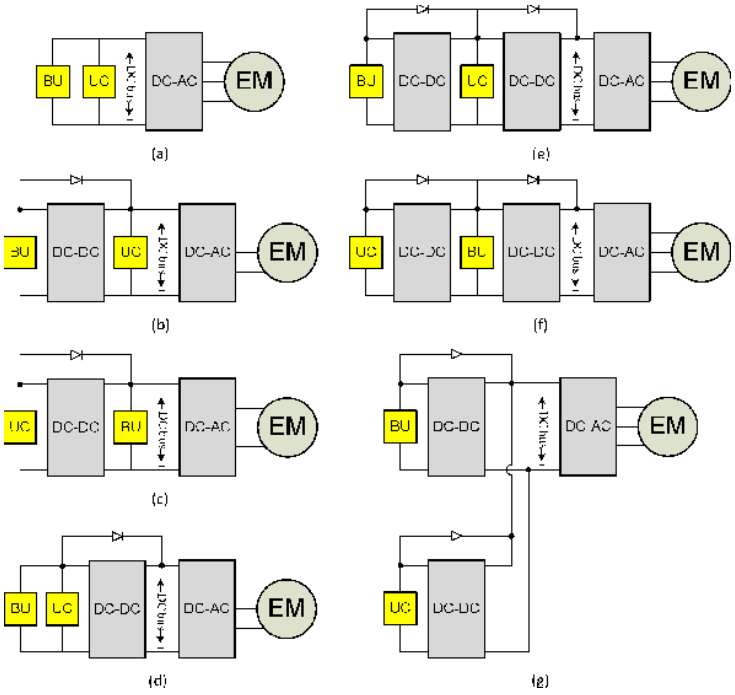

Figure 1.6: Different configurations of interfacing BU and SC to the DC bus in a drive train

1.8 Driving cycles for electric vehicles

A driving cycle is a standardized representation of vehicle speed points over a specific time period. It is used to evaluate fuel consumption and emissions in a consistent manner, allowing for comparisons between different vehicles. Typically, driving cycles are conducted on chassis dynamometers, where exhaust emissions are measured to assess emission rates.

In the context of commercial vehicles, driving cycles are performed on engine dynamometers, and the evaluation is based on a set of engine torque and speed points rather than vehicle speed points. This approach enables the assessment of engine performance and emissions characteristics.

There are two main types of driving cycles: modal cycles and transient cycles. Modal cycles, such as the European standard NEDC (New European Driving Cycle) and the Japanese 10-15 Mode, consist of a series of fixed acceleration and constant speed periods. However, these modal cycles do not accurately represent real-world driving behavior since they do not incorporate the typical variations in speed that occur on the road.

On the other hand, transient cycles, such as the FTP-75 (Federal Test Procedure-75) or Artemis cycle, involve a wide range of speed variations, better reflecting the driving conditions encountered in real-world scenarios. These cycles are designed to capture the dynamic nature of driving with frequent speed changes [23].

1.8.1 Japanese driving cycle

Figure 1.7 illustrates a 10-mode driving cycle designed to simulate urban driving conditions. This particular segment covers a distance of 0.644 kilometers with an average speed of 17.7 kilometers per hour. The driving cycle presented in Figure 1.7 serves as the basis for the subsequent simulations and analyses conducted in this study, capturing the characteristic driving patterns encountered in urban areas. It provides a representative profile of speed variations and acceleration periods that are reflective of typical urban driving scenarios. By utilizing this driving cycle, we aim to evaluate the performance and efficiency of the hybrid electric vehicle system under realistic operating conditions [24].

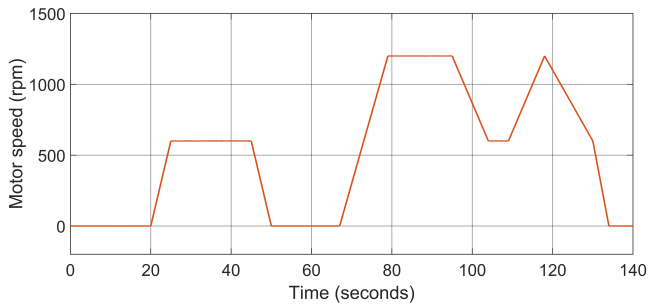

Figure 1.7: Japnese driving cycle

1.9 Energy management

Energy management in vehicles is an important issue because it can significantly influence the vehicle's performance. An optimal energy management strategy can provide substantial advantages such as reducing fuel consumption, decreasing emissions, reducing pollution, and improving vehicle driving performance [25].
Recently, research has focused on improving EMS (energy management strategies) because of its complexity and limitless capacities. So, depending on the driving cycle and storage condition, EMS must be reconfigurable [26].
EMSs can be divided into: Rule-Based (RB) and Optimization-Based (OB).

1.9.1 Rule-Based EMSs

Rule-based EMSs can typically be implemented by predefining the logical rules in accordance with the HEV system characteristics and operation mode. Through an "if-then" structure, the rules are determined depending on the battery SOC, driver power demand, and vehicle velocity. Given these guidelines, the power split can be carried out to meet the driver's power demand while keeping the SOC within a predetermined range. This strategy primarily relies on logical rules and local restrictions rather than prior knowledge of the driving cycle. It is less flexible to changing driving conditions since the control parameters cannot be modified due to a lack of future knowledge on the driving cycle. The next sequel introduces common techniques, such as deterministic rule-based control and fuzzy rule-based methods [27].

Deterministic Rule-Based EMSs

This approach involves using the engine map and motor efficiency map to determine how power should be distributed between the engine and motor. By considering the efficiency of both the motor and engine, as well as the battery state of charge (SOC), a set of predefined logical rules is used to allocate power. These control rules can be easily implemented in real-time using a look-up table, making them popular for vehicle controllers in commercial applications. Typically, the rules are designed based on specific driving cycles, such as the ECE cycle. However, the effectiveness of this method may be reduced when faced with varying traffic conditions, limiting its adaptability to different driving cycles [27].
introduce a rule-based Energy Management System (EMS) for a parallel hybrid electric vehicle. However, traditional rule-based power management systems are not ideal for real-world driving conditions because there is no single standardized approach for designing the logical rules. Typically, this process relies on the engineer's expertise and specific driving cycles. The subsequent sections provide a more comprehensive discussion on rule-based strategies, specifically the on/off and power follower EMSs [27]. Rule-based EMSs are easy to implement online but lack optimality and cannot guarantee optimal performance for various driving cycles. Additionally, they are unable to adjust control parameters to achieve optimal fuel economy due to the complexity of driving conditions [27].

Fuzzy Logic-Based EMSs

Fuzzy logic control theory is a methodology that combines fuzzy set theory and fuzzy logic to determine system output. It goes beyond traditional TRUE and FALSE logic by incorporating fuzzy rules. In the context of Energy Management Systems (EMSs), fuzzy logic-based approaches are used to distribute power based on fuzzy rules that consider driver power demand and State of Charge (SOC). Modified versions of fuzzy logic-based EMSs are also utilized, such as fuzzy logic controllers for parallel Hybrid Electric Vehicles and multi-input fuzzy logic controllers for power-split hybrid vehicles.

The utilization of fuzzy logic-based EMSs in energy management offers advantages over traditional rule-based systems, including enhanced fuel efficiency and the ability to adapt to different driving conditions. Several researchers have proposed innovative approaches that leverage fuzzy logic controllers to optimize power distribution and reduce emissions

in various vehicle applications. These advancements highlight the potential of fuzzy logic control theory in the field of energy management for electric and hybrid vehicles [27].

1.9.2 Global Optimization-Based EMSs

Global Optimization-Based EMSs refer to energy management systems that utilize global optimization techniques to optimize the energy consumption and operation of a system. These systems are typically used in complex energy systems, such as smart grids, micro-grids, or hybrid energy systems, where multiple energy sources and storage devices need to be coordinated to achieve efficient and optimal operation.

The primary goal of a Global Optimization-Based EMS is to minimize the overall energy cost or maximize the system's performance while considering various constraints, such as power generation limits, storage capacity, demand response, and environmental factors. The optimization problem involves finding the optimal scheduling and dispatch strategies for different energy resources to meet the energy demand in the most efficient manner.

Global optimization techniques, such as Mixed Integer Linear Programming (MILP), Genetic Algorithms (GA), Particle Swarm Optimization (PSO), or Simulated Annealing (SA), are employed to solve the complex optimization problems associated with EMSs. These techniques explore the entire solution space to find the global optimum, considering the non-linear and non-convex nature of the problem. [27].

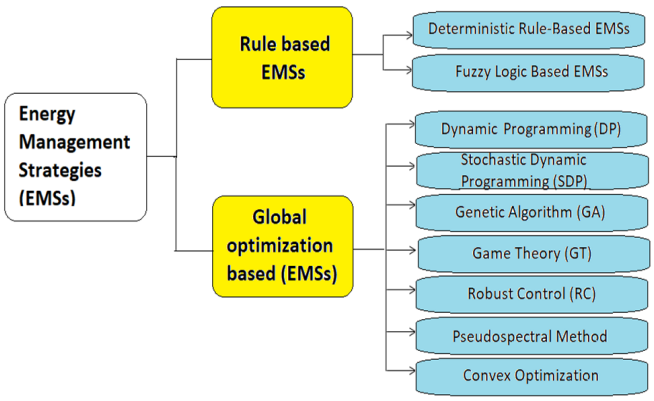

Figure 1.8: Types of Energy Management Strategies

Figure 1.8 illustrates a comprehensive overview of various energy management strategies.

1.10 Conclusion

In conclusion, the first chapter delves into the key aspects of electric vehicles and hybrid electric vehicles, shedding light on their historical background, architectural design, technological advancements, energy storage options, types of electric motors used, and the importance of efficient energy management. By understanding these fundamental concepts, we lay the groundwork for exploring advanced control strategies and optimization methods in the subsequent chapters. The comprehensive overview provided in this chapter sets the stage for a deeper understanding of the complexities and challenges involved in achieving optimal energy utilization in hybrid electric vehicles.

Chapter 2

Modeling of different traction chain elements

2.1 Introduction

In this chapter, we will present a comprehensive analysis of the chosen system architecture, followed by the modeling of its various subsystems.

The first section focuses on presenting a detailed model of the power sources employed in the system. This includes modeling the battery, which serves as the primary power source, and the Super-capacitor module, utilized as a secondary power source .

Moving on to the second section, our attention is directed towards the conversion stage. Here, we explore three power converters that were utilized to validate energy management strategies and verify control rules for the traction section. Specifically, Boost converter is selected for the battery, while an Buck-Boost converter is employed for the Super-capacitor. Additionally, a two-level, three-phase voltage inverter is utilized as a variable speed drive, enabling us to verify the control rules for the traction section.

Lastly, the third section revolves around the vehicle's traction system. In this section, we model the BLDC motor, taking into account various forces that impact the vehicle's dynamics. Through the systematic exploration of the system architecture and the detailed modeling of key subsystems, this chapter aims to enhance our understanding of hybrid electric vehicle systems and lay the groundwork for further analyses, optimizations, and advancements in the field. Figure 2.1 illustrates the porposed full active traction chain topology.

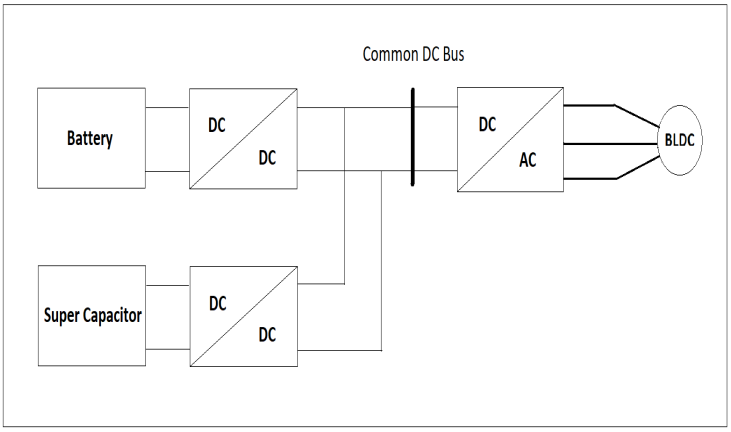

Figure 2.1: Proposed Topology for the Hybrid Electric Vehicle System

2.2 Mathematical model of hybrid energy storage system

The mathematical model of a hybrid energy storage system (HESS) combines the dynamic equations of the different components within the system to describe its behavior. The HESS typically consists of multiple energy sources, such as batteries, super-capacitors along with power electronics converters and loads.

2.2.1 Thevenin based battery model

The primary energy source used in this electric vehicle is the Lithium-ion battery. For modeling purposes, the Lithium-ion battery is represented using the well-known one branch Thevenin scheme. This model accurately captures the behavior of the battery. Figure 2.2 illustrates the equivalent circuit of the Thevenin-based battery model [28].

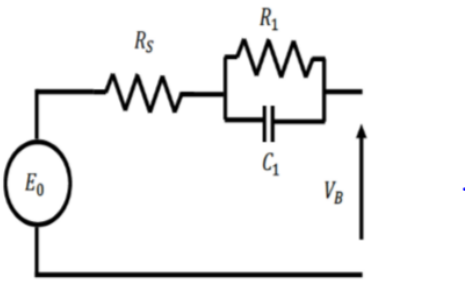

Figure 2.2: The equivalent circuit of Thevenin based battery model.

In this representation, the open circuit voltage E0 represents the voltage of the bat-

tery when no current is flowing. The voltage drop across the internal resistance Rbatt accounts for the Joule losses in the battery. The dipole formed by R1 and C1 represents the stored energy in the battery [28].

$$V_{\text{batt}} = E_0 - V_1 - R_{\text{batt}} \cdot I_{\text{batt}} \tag{2.1}$$

The equation 2.1 describes the relationship between the battery voltage (Vbatt), the open circuit voltage (E0), the voltage drop across R1 (V1), the battery internal resistance (Rbatt), and the battery current (Ibatt).

The state of charge (SOC) estimation of each battery is calculated using the Coulomb counting method. It involves integrating the discharge current (i(t)) over a period from T0 to Tf and dividing by the nominal capacity of the battery (Cn). The initial state of charge (SOC0) is subtracted from this value, and the result is multiplied by 100 to obtain the SOC in percentage [28].

$$\text{SOC}(\%) = \text{SOC}_0 - \frac{1}{C_n} \int_{T_0}^{T_f} i(t)\, dt \times 100 \tag{2.2}$$

where:

$$\begin{aligned} \text{SOC}_0 &= \text{Initial state of charge} \\ C_n &= \text{Nominal capacity of the battery expressed in (Ah)} \\ i(t) &= \text{Discharge current} \end{aligned}$$

In essence, this method calculates the change in state of charge by considering the difference between the initial state of charge and the integrated current over a specific time period (T_0) to T_f).

2.2.2 Super-capacitor RC based model

The super-capacitor simulation involves utilizing a conventional RC circuit. In this approach, the super-capacitor is represented as an ideal capacitor connected in series with a resistor. The resistor corresponds to the internal resistance of the super-capacitor, which accounts for the joule losses within the device. The RC circuit configuration [28], shown

in Figure 2.3, serves as the model for the super-capacitor simulation.

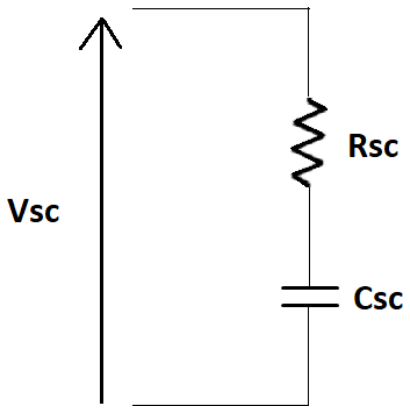

Figure 2.3: The equivalent circuit of super-capacitor R-C based model

In the RC circuit model, several variables are defined as follows:

V_{sc0} : Voltage across the ideal capacitor

V_{sc} : Terminal voltage of the super-capacitor

I_c : Output current of the super-capacitor

Based on the RC circuit, the terminal voltage of the super-capacitor Vsc can be expressed using the equation:

$$V_{sc} = V_{sc0} - R_{sc} \cdot I_c \tag{2.3}$$

The variable C represents the stored energy amount and is given by:

$$C = C_0 + V_{sc0} \cdot K \tag{2.4}$$

where:

R_{sc}: the internal resistance of the super-capacitor.

I_{sc}: the current flowing through the super-capacitor.

C_0: a constant representing the initial stored energy.

K: a constant factor.

These equations describe the relationship between the voltage, current, and stored energy in the super-capacitor within the RC circuit model.

2.2.3 DC-DC converter model

To ensure bidirectional energy flow between the involved sources according to the adopted control strategy, the converter structures used are current-reversible topologies.

The Buck-Boost converter model on the SC side

Referring to Figure 2.4, the continuous dynamic model of the Buck-Boost converter used for the super-capacitor can be obtained by combining the switching modes as follows [28]:

In the Buck mode, where S1=1 and S2=0, the following expressions are derived for the energy storage elements L_{SC} and C:

$$L_{SC} \cdot \frac{di_{\mathrm{SC}}}{dt} = V_{\mathrm{SC}} - V_{\mathrm{DC}} \tag{2.5}$$

$$C \cdot \frac{dV_{\mathrm{DC}}}{dt} = i_{\mathrm{Lsc}} - \frac{V_{\mathrm{DC}}}{R_{\mathrm{L}}} \tag{2.6}$$

In the Boost mode, where S1=0 and S2=1, the following expressions can be expressed as:

$$L_{SC} \cdot \frac{di_{\mathrm{SC}}}{dt} = V_{\mathrm{SC}} \tag{2.7}$$

$$C \cdot \frac{dV_{\mathrm{DC}}}{dt} = i_{\mathrm{Lsc}} \tag{2.8}$$

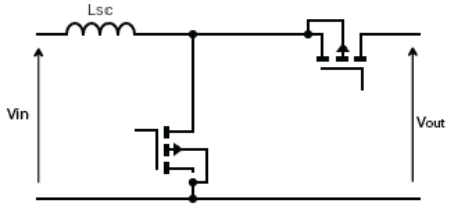

Figure 2.4: The equivalent circuit of the Buck-Boost converter

The Boost converter model on the Battery side

The mathematical modeling begins with storage elements capacitor and inductor in the boost converter as shown in Fig 2.5. inductor voltage and capacitor current are given in eqn 2.9 and 2.10 respectively [29].

$$V_L = L \cdot \frac{di_L}{dt} \tag{2.9}$$

$$i_C = C \cdot \frac{dV_C}{dt} \tag{2.10}$$

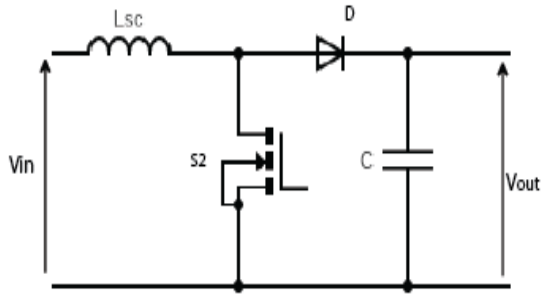

Figure 2.5: The equivalent circuit of the Boost converter

The boost conversion begins when the switching process starts,which results in two forms of switching conditions MOSFET ON and MOSFET OFF.

2.2.4 DC bus model

In the literature, two types of interconnections exist for stationary and embedded hybrid systems: the architecture with alternating node interconnection and the one with continuous node, as proposed in this work. The main advantage lies in not requiring synchronization between the different included entities. In this work, the two sources are interconnected through a continuous bus, whose voltage needs to be regulated around a reference value. This reference value is determined based on the converter voltage ratio and the machine used. This regulation allows for the collection of energy flows from both sources and their delivery to the traction motor, while maintaining a stable voltage at the input of the voltage inverter [28]. Figure 2.6 shows the continuous bus capacitor,

which transfers all the currents from the continuous side to the machine through the I_DC current, representing the BLDC motor current in the continuous side.

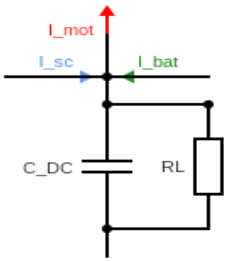

Figure 2.6: The equivalent diagram of the DC bus

In conclusion, by utilizing average models of the converters, the model of the continuous bus can be expressed as follows:

$$C_{\mathrm{DC}}\frac{dV_{\mathrm{DC}}}{dt} = I_{\mathrm{SC}} \cdot a_{\mathrm{SC}} + I_{\mathrm{Batt}} \cdot a_{\mathrm{Batt}} - \frac{V_{\mathrm{DC}}}{R_{\mathrm{L}}} - I_{\mathrm{mot}} \tag{2.11}$$

2.2.5 Inverter model

The three-phase inverter is an important part of the system, consisting of six power switches. Each phase leg is connected to two switches, forming a bridge configuration. These switches are responsible for controlling the power flow to the three-phase BLDC motor [30].

In this particular configuration, the power switches of the inverter are connected to a combination of a battery and a super-capacitor, which are connected in parallel. This arrangement allows for efficient energy storage and supply to the motor. Figure 2.7 shows the voltage source inverter connected to the BLDC motor

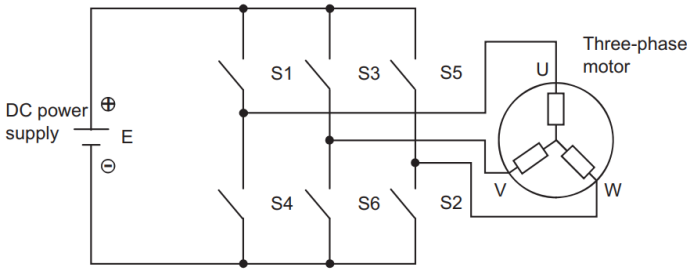

Figure 2.7: Three-phase inverter basic circuit

Table 2.1 provides a detailed overview of the timing intervals for each gating signal.

Each interval corresponds to a 60° segment of the motor cycle. Within each interval, the corresponding MOSFET conducts for a duration of 120° [30].

The design of the inverter is based on logical equations (2.5), (2.6), and (2.7), which determine the logical state of each switch (S_1 to S_6). A logical value of 1 represents the switch being turned ON, while a logical value of 0 represents the switch being turned OFF.

By applying these logical equations and following the timing sequence specified in Table 2.1, the inverter controls the switching patterns of the power switches. This ensures that each MOSFET conducts for the designated duration, allowing for the proper modulation of the input voltage to the three-phase BLDC motor [30].

Overall, the use of logical equations and precise timing intervals enables efficient and reliable operation of the inverter circuit in controlling the power flow to the motor.

$$V_a = S_1\frac{V_d}{2} - S_4\frac{V_d}{2} \tag{2.12}$$

$$V_b = S_3\frac{V_d}{2} - S_6\frac{V_d}{2} \tag{2.13}$$

$$V_c = S_5\frac{V_d}{2} - S_2\frac{V_d}{2} \tag{2.14}$$

Where: V_d is the DC-link voltage.

Phase Voltage	Switch States		Output Voltage
	ON	OFF	
V_a	S_1	S_4	$+V_d/2$
	S_4	S_1	$-V_d/2$
V_b	S_3	S_6	$+V_d/2$
	S_6	S_3	$-V_d/2$
V_c	S_5	S_2	$+V_d/2$
	S_2	S_5	$-V_d/2$

Table 2.1: Switching states

2.2.6 Mathematical model of BLDC motor

BLDC motors are a type of synchronous motor that offers advantages such as reduced rotor Ohmic losses and the absence of brushes and mechanical commutation. Unlike traditional DC motors, BLDC motors have a permanent magnet rotor and wire-wound stator poles. Due to the absence of brushes, these motors require an inverter and a rotor

position sensor for operation [30].

Hall Effect sensors are commonly used to detect the position of the rotor in BLDC motors. In self-control mode, the inverter functions as an electronic commutator, receiving switching logical pulses from the absolute position sensors. This control mechanism is also referred to as electronic commutation. The type of inverter used depends on the power rating of the drive, with transistors typically used for low-power drives and thyristors for high-power drives. The Hall Effect sensor is mounted on the motor shaft [30], as depicted in the following figure:

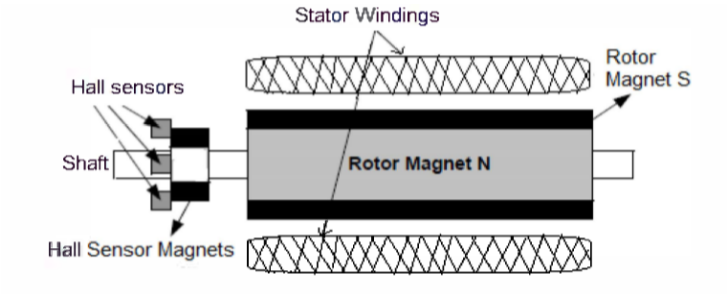

Figure 2.8: The construction of a conventional BLDC motor

This configuration allows for accurate rotor position detection, enabling precise control of the BLDC motor's operation.

The rotor magnetic poles of the BLDC motor emit either a high or low signal as they pass close to the Hall sensor. This signal indicates whether the north or south pole is passing by the sensor. By analyzing the combination of signals from the three Hall sensors, the precise commutation sequence can be computed. This commutation sequence signal is then transmitted to the drive circuitry of the inverter circuit, enabling the controlled flow of current to the stator phase windings [30].

Table 2.2 shows the Hall Effect signal values, which provide information about the states of the magnetic poles and assist in determining the commutation sequence.

The Hall Effect signals play a main role in achieving proper motor operation and ensuring the correct timing of current commutation in the stator windings. By accurately sensing the rotor position, the inverter circuit can control the switching of the power switches to maintain the desired torque and speed of the motor [30].

Switching Interval Degree	H1	H2	H3
0-60	1	0	1
60-120	0	0	1
120-180	0	1	1
180-240	0	1	0
240-300	1	1	0
300-360	1	0	0

Table 2.2: Hall Effect signals

Based on the Hall Effect signals, the inverter controls the current flow to the stator phase windings, allowing the BLDC motor to operate at the desired torque and speed.

The equivalent circuit of the BLDC motor, as shown in Figure 2.9, consists of three stator-phase windings connected in a star pattern and a permanent magnet mounted on the rotor. The motor is powered by a three-phase voltage source, which can be applied as a square wave, sinusoidal wave, or any other waveform.

When modeling the BLDC motor, several assumptions are made [30]:

(i) The motor operates with the rated current and is not saturated.

(ii) The resistances of the three stator phase windings are equal.

(iii) Self-inductance and mutual inductance remain constant

(iv) Iron and stray losses are negligible.

(v) The three phases are balanced.

(vi) The air gap is uniform.

(vii) Hysteresis and eddy current losses are not considered.

(viii) Semiconductor switches are assumed to be ideal.

These assumptions help simplify the modeling process and provide a basis for analyzing the motor's behavior and performance.

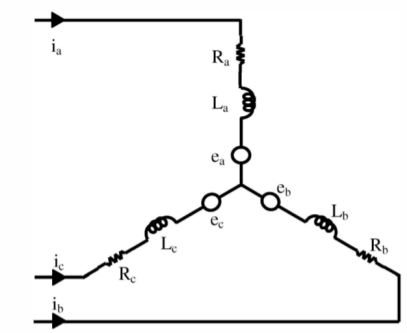

Figure 2.9: The equivalent circuit of the BLDC motor

$$V_a = R_a \cdot i_a + L_a \cdot \frac{di_a}{dt} + e_a \tag{2.15}$$

$$V_b = R_b \cdot i_b + L_b \cdot \frac{di_b}{dt} + e_b \tag{2.16}$$

$$V_c = R_c \cdot i_c + L_c \cdot \frac{di_c}{dt} + e_c \tag{2.17}$$

where: $R_a = R_b = R_c = R$: Stator resistance per phase [Ohm]

$L_a = L_b = L_c = L$: Stator inductance per phase [Henry]

V_a, V_b, and V_c are the stator phase voltages [Volt]

i_a, i_b, and i_c are the stator phase currents [Ampere]

e_a, e_b, and e_c are the motor back EMFs, and their expressions will be given in equations (2.11), (2.12), and (2.13).

$$\begin{pmatrix} V_a \\ V_b \\ V_c \end{pmatrix} = \begin{pmatrix} R + pL & 0 & L_c \\ L_a & R + pL & 0 \\ 0 & L_b & R + pL \end{pmatrix} \begin{pmatrix} i_a \\ i_b \\ i_c \end{pmatrix} + \begin{pmatrix} e_a \\ e_b \\ e_c \end{pmatrix}$$

where p in the matrix represents $\frac{d}{dt}$.

When a BLDC motor rotates, each winding generates a voltage known as Back EMF (Electromotive Force), which opposes the main voltage supplied to the winding according to Lenz's law. The polarity of the Back EMF is in the opposite direction to the source voltage. The Back EMF is related to the rotor position, and each phase has a phase difference of 120° [30].

The equation of the ideal Back EMF and phase current for each phase of the motor can be expressed as follows:

$$e_a = K \cdot \omega \cdot f(\theta) \tag{2.18}$$

$$e_b = K \cdot \omega \cdot f(\theta - \frac{2\pi}{3}) \tag{2.19}$$

$$e_c = K \cdot \omega \cdot f(\theta + \frac{2\pi}{3}) \tag{2.20}$$

where:

K is the Back EMF constant [V/rad/s],

θ is the electrical rotor angle

ω is the mechanical speed of the rotor [rad/s],

and $f(\theta)$ is a function related to the rotor position.

The electromagnetic torque can be expressed as:

$$T_e = J \cdot \frac{d\omega}{dt} + T_l + B \cdot \omega \tag{2.21}$$

where:

J is the rotor inertia [kg·m^2],

$\frac{d\omega}{dt}$ is the rate of change of mechanical speed,

T_l is the load torque [N·m],

and B is the damping constant.

The resultant torque can be calculated as:

$$T_e - T_l = J \cdot \frac{d\omega}{dt} + B \cdot \omega \tag{2.22}$$

This represents the relationship between the electromagnetic torque, load torque, rotor inertia, mechanical speed, and damping constant in the BLDC motor.

2.2.7 Dynamic model of electric vehicle

During the operation of a vehicle, it encounters several resistance forces that oppose its forward motion. These forces are essential to consider when analyzing the vehicle's dynamics and energy consumption [31]. The resistance forces can be categorized as follows:

Wind Resistance (F_W):

Wind resistance is the force experienced by the vehicle due to the interaction between its shape and the surrounding air. It is influenced by factors such as the vehicle's aerodynamic design, speed, frontal area, and air density. At higher speeds or for vehicles with poor aerodynamics, wind resistance becomes a significant factor contributing to the total resistance.

Rolling Resistance (F_R):

Rolling resistance refers to the force required to overcome the friction between the tires and the road surface. It is influenced by various factors, including tire type, tire

pressure, road conditions, and vehicle weight. Improper tire inflation or using tires with higher rolling resistance can increase this resistance, resulting in decreased fuel efficiency.

Grade Resistance (F_G): Grade resistance is the force encountered when a vehicle travels on an incline or decline. It depends on the road gradient and the weight of the vehicle. When driving uphill, the vehicle needs additional energy to overcome gravity and maintain its speed. Conversely, when traveling downhill, the vehicle experiences a negative grade resistance that can assist in maintaining or increasing its speed.

Acceleration Resistance (F_A): Acceleration resistance is the force required to accelerate the vehicle from rest or change its velocity. It is directly proportional to the mass of the vehicle and the desired rate of acceleration. To overcome this resistance, the engine or motor must provide sufficient power to accelerate the vehicle.

The total tractive force (F_T) acting on the vehicle can be obtained by summing up these resistance forces [31]

$$F_T = F_W + F_R + F_G + F_A \tag{2.23}$$

$$F_T = K_R \cdot W \cdot \cos(\delta) + K_W \cdot A \cdot V^2 + W \cdot \sin(\delta) + W \cdot \frac{a}{g} F_T \tag{2.24}$$

K_R : Rolling resistance coefficient

K_W : Wind resistance coefficient

δ : Road grade angle

W : Vehicle weight

V : Vehicle speed

A : Vehicle frontal area

a : Vehicle acceleration

g : Gravitational constant

Understanding and quantifying these resistance forces are crucial for vehicle performance analysis, energy consumption estimation, and the design of efficient propulsion systems. By considering the interplay between these forces, engineers and researchers can optimize vehicle performance and improve overall energy efficiency.

In Figure 2.10, a graphical representation of the total tractive force is depicted, illustrating the combined effects of wind resistance, rolling resistance, grade resistance, and

acceleration resistance. This visualization aids in comprehending the relative contributions of each force and their impact on the overall vehicle dynamics.

In summary, the detailed analysis and consideration of wind resistance, rolling resistance, grade resistance, and acceleration resistance provide valuable insights into the challenges faced by a moving vehicle and serve as a foundation for optimizing vehicle performance and energy efficiency.

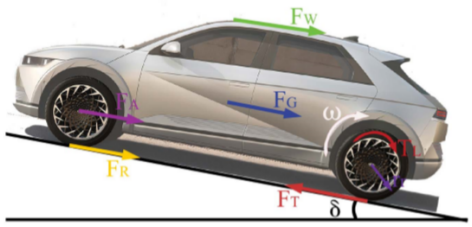

Figure 2.10: Vehicle dynamic model for resistance forces calculation

Once the tractive force F_T has been calculated, the operating point parameters of the motor, including speed ω, torque τ_L, and power P_L, can be computed using the following equations [31]:

$$\omega = \frac{W^*}{r} \tag{2.25}$$

$$\tau_L = \frac{r}{W^*} \cdot F_T \tag{2.26}$$

$$P_L = F_T \cdot \omega \tag{2.27}$$

where:

W^* is the angular velocity of the motor,

r is the effective radius of the wheel,

F_T is the tractive force.

These equations provide the relationship between the tractive force and the operating point parameters of the motor.

2.3 Conclusion

This chapter focused on describing and modeling the various components of the hybrid system. Each component was carefully selected to ensure an appropriate model for its

operation. The chapter began with a detailed description and modeling of the lithium-ion battery pack, taking into account its specific characteristics and behavior. The next component, the super-capacitor, was also thoroughly described and modeled, considering its unique properties and functionalities within the system. Lastly, the different power converters used for power flow control within the system were modeled, taking into consideration their role in optimizing the system's performance. By accurately modeling each component, a comprehensive understanding of the hybrid system and its overall operation can be achieved.

Chapter 3

Control of Traction chain

3.1 introduction

The control of the traction chain in Electric Vehicles (EVs) is important for achieving efficient and reliable performance. This chapter focuses on presenting various control strategies and techniques that are employed to regulate and optimize the traction chain in EVs.

Firstly, the implementation of the control for the Hybrid Energy Storage System (HESS) with DC/DC converters is decribed in this chapter. It explores how fuzzy logic can effectively regulate and optimize the performance of the HESS.

Secondly, the chapter dives into the energy management strategy, which encompasses the definition of operating modes and the design of a fuzzy logic controller. These elements are important for achieving efficient energy distribution and maximizing the overall performance of the EV.

Lastly, the chapter delves into the control of Brush-less DC Motors (BLDC) in EVs. It specifically examines two control techniques: hysteresis current control and TS-FLC speed control. These techniques enable precise speed regulation and enhance the motor's overall performance in EVs.

3.2 HESS control using fuzzy logic controller

In a hybrid electric vehicle (HEV), the control loops associated with the power sources, namely the battery and super-capacitor, play an essential role in managing the power flow

and ensuring optimal operation. These control loops involve the use of DC/DC converters, specifically boost and buck-boost converters, to connect the battery and super-capacitor to the inverter's DC bus.

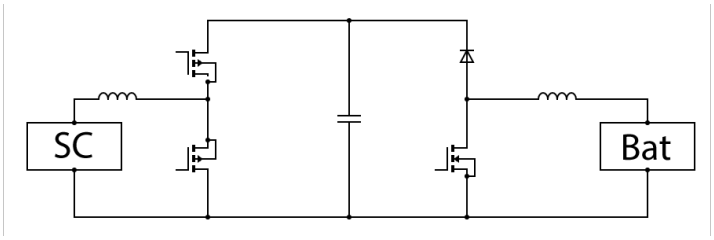

(a)

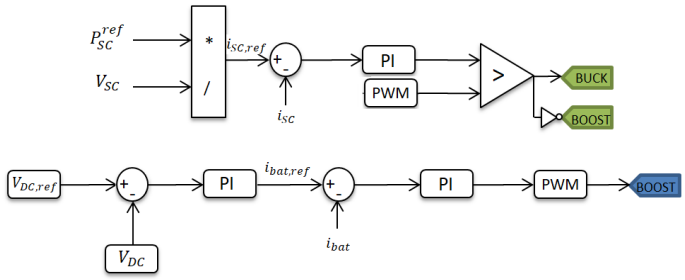

(b)

Figure 3.1: Power sources and their corresponding control loops

The control loop for discharging the battery in the hybrid electric vehicle system involves comparing the DC bus voltage V_{DC} with a reference voltage V_{DC}. The resulting error signal is used as input to a PI controller, which determines the battery current reference.

The battery current reference is then compared with the actual battery current, generating an error signal. This error signal is controlled by a PWM generator, which adjusts the duty cycle of the converter. By continuously monitoring and adjusting the duty cycle based on the error signal, the control loop ensures that the battery current closely matches the desired reference value. This control mechanism helps maintain the stability of the battery's voltage and optimizes the power transfer from the battery to the DC bus

In the control loop of the super-capacitor,the power reference is divided by the super-capacitor voltage to determine the current reference. By comparing the measured current with the reference, an error signal is generated.

To control the power flow, a buck-boost converter is utilized, controlled by a PWM

generator. If the measured current is lower than the reference, indicating insufficient power, the duty cycle of the converter is increased to boost the voltage across the super-capacitor and enhance the current flow. Conversely, if the measured current exceeds the reference, the duty cycle is reduced to decrease the voltage and limit the current flow.

The control loop continuously monitors the error signal using a PI controller to adjust the duty cycle accordingly, ensuring efficient power transfer and optimal utilization of the super-capacitor's energy. This helps maintain a stable voltage level and improves the overall performance of the hybrid electric vehicle system

3.3 Description of Energy Management strategy

3.3.1 Operating modes

In an Electric Vehicle (EV), a Hybrid Energy Storage System (HESS) operates in different modes to effectively manage energy. These modes determine how the battery and super-capacitor work together based on the vehicle's speed and driving conditions. In this work we distinct four operating states:

Mode 0: In this mode, when the vehicle speed is zero, both the battery and super-capacitor are turned off. This means that no power is being supplied or stored in either of these energy storage components.

Mode 1: When the vehicle is moving at a constant speed, the battery is turned on and supplying power to the BLDC motor. However, the super-capacitor remains off, meaning it is not actively participating in providing or storing electrical energy.

Mode 2: During acceleration, both the battery and super-capacitor are turned on. This means that both energy storage systems are working together to provide the necessary power to the BLDC motor, enabling the vehicle to accelerate efficiently.

Mode 3: During deceleration, the super-capacitor comes into play. It is utilized to capture and store the electrical energy generated by regenerative braking. As the vehicle slows down, the super-capacitor charges up, effectively recovering and storing some of the energy that would have been wasted as heat in traditional braking systems.
By intelligently switching between different modes, the electric vehicle can optimize its energy usage and enhance overall efficiency.

3.3.2 Design of the Fuzzy logic energy management system

To validate the proposed energy management strategy, we created an optimal energy management strategy using fuzzy logic. This strategy uses a fuzzy power management algorithm that determines the reference power for the super-capacitor based on factors such as power demand, super-capacitor state of charge (SOC), and the rate of change of power over time. The battery's SOC is not considered when making these decisions. Additionally, by carefully selecting rules in the fuzzy table, we achieve intelligent power distribution without requiring extra filters.

The fuzzy logic controller (FLC) shown in Figure 3.2 determines the reference power that will be delivered by the SC. To do so, the super-capacitor state of charge, the power demand and its slop are fuzzified using adequate membership functions.

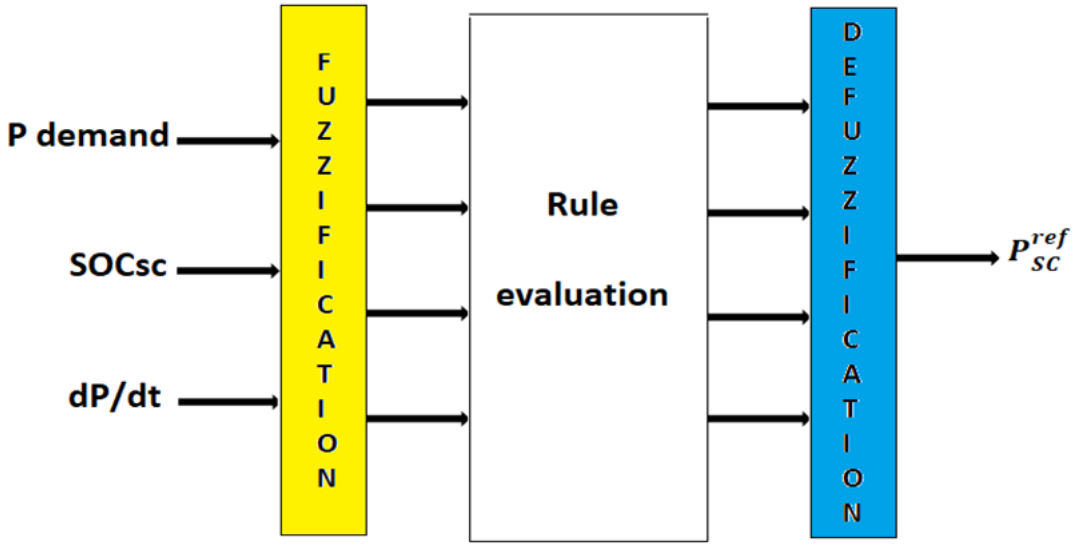

Figure 3.2: The fuzzy logic controller

In Figure 3.3, three membership functions of triangular and trapezoidal types are depicted. These membership functions are employed to fuzzify the power demand variable. The power demand is divided into three fuzzy sets: low power (L), medium power (M), and high power (H).

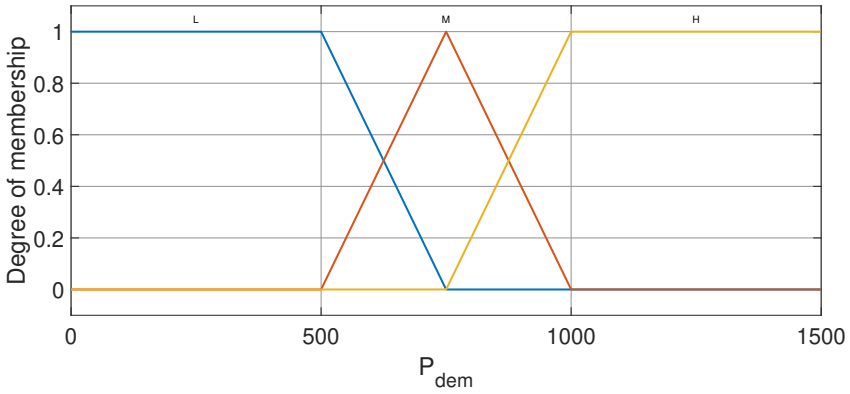

Figure 3.3: The fuzzification of the power demand

Figure 3.4 illustrates the membership functions employed to fuzzify the state of charge (SOC) of the super-capacitor. These membership functions are used to convert the crisp value of the super-capacitor SOC into linguistic terms or fuzzy variables.

The SOC of the super-capacitor is divided into three fuzzy sets: low SOCsc (L), medium SOCsc (M), and high SOCsc (H). Each fuzzy set is associated with a membership function that defines its boundaries and shape.

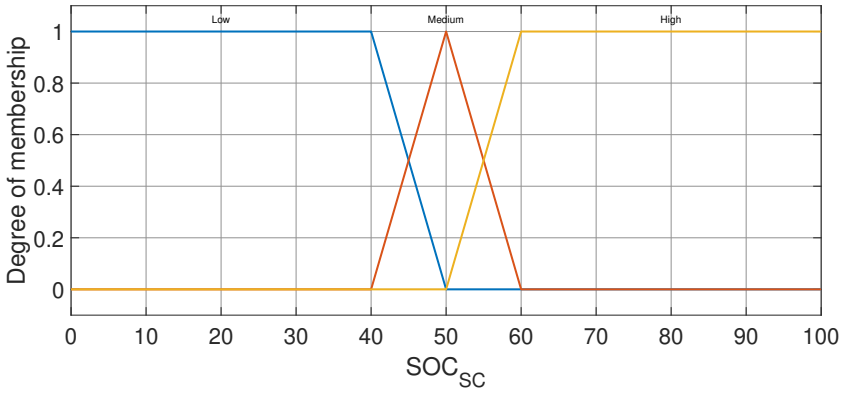

Figure 3.4: The supercapacitor SOC fuzzification

Figure 3.5 presents the membership functions utilized to fuzzify the derivative of the power demand.

The derivative of the power demand is divided into three fuzzy sets: Negative slope (N), Zero slope (Z), and Positive slope (P).

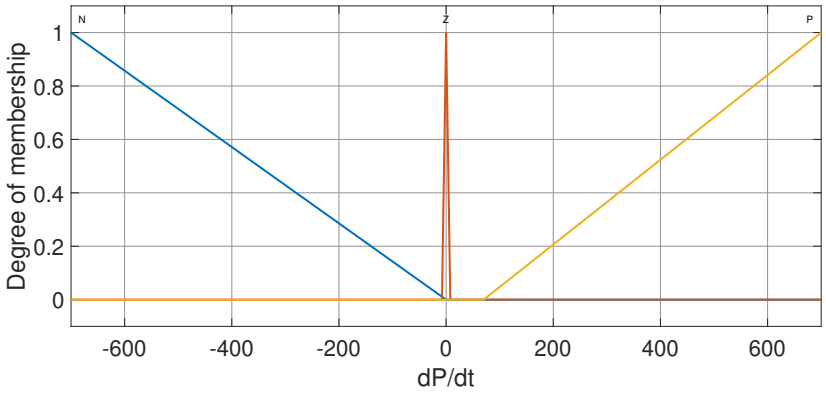

Figure 3.5: The slop of power demand fuzzification

The control system for the supercapacitor utilizes six triangular membership functions, as depicted in Figure 3.6, to represent the reference power. These membership functions, including Very Negative (VN), Negative (N), Zero (Z), Low (L), Medium (M), and High (H), cover a wide range of power values, from highly negative to high levels.

By using these membership functions, the control system can linguistically describe and interpret the desired power level for the super-capacitor. This enables the application of fuzzy logic control algorithms to adjust the power flow and ensure optimal operation of the hybrid energy storage system.

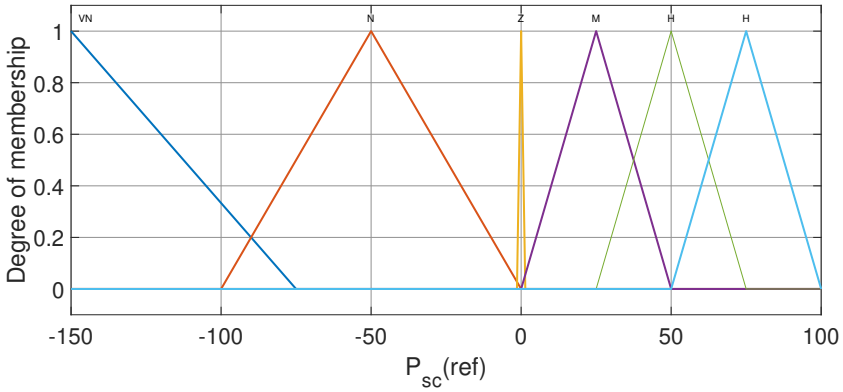

Figure 3.6: The defuzzification of the supercapacitor's reference power

The fuzzy logic controller in the system utilizes a set of 27 predefined combinations to effectively control the state of charge (SOC) of the super-capacitor, power demand, and its derivative, as outlined in Table 3.1. These combinations enable the controller to make intelligent decisions and adjust the system's parameters for optimal performance. By interpreting linguistic variables and corresponding rules, the controller regulates the

SOC, adjusts power demand, and responds to changes in power demand's derivative. This approach provides a robust and adaptable control strategy, enhancing the overall performance of the super-capacitor.

Pdem		L	M	H
SOCsc	dp/dt			
L	N	N	VN	VN
	Z	Z	Z	Z
	P	Z	L	L
M	N	N	N	VN
	Z	Z	Z	Z
	P	L	L	M
H	N	N	N	N
	Z	Z	Z	Z
	P	L	M	H

Table 3.1: The Fuzzy logic energy management rules base

3.4 Control Strategies for Brushless DC (BLDC) Motors

To achieve optimal efficiency in controlling a BLDC motor, it is essential to have continuous knowledge of the rotor position. This can be achieved through two different modes: sensor mode and sensorless mode.

In the sensor mode, information about the rotor position is obtained from Hall Effect sensors, with one sensor per phase. These sensors provide feedback based on the motor's magnetic field. On the other hand, in the sensorless mode, the rotor position is determined by analyzing the Back Electromotive Force (BEMF) signals generated by the motor. The type of BEMF waveform produced by the motor can be either trapezoidal or sinusoidal, depending on the arrangement of windings in the stator. Distributed windings result in a sinusoidal BEMF, while concentrated windings produce a trapezoidal BEMF.

In both modes, the commutation of the BLDC motor is carried out using electronic switches that require knowledge of the rotor position. By aligning the rotor poles with the stator windings, the corresponding stator windings can be energized. A predefined commutation interval is used to drive the motor effectively. However, precise speed control and maximum torque generation can only be achieved by performing brushless commutation with accurate rotor position information.

Mechanical position sensors such as Hall sensors, shaft encoders, or resolvers have traditionally been utilized in control methods that rely on sensors to provide rotor position information.

3.4.1 BLDC control using Hysteresis comparators

Hysteresis control is a simple closed-loop control technique commonly used in motor control. It involves maintaining the controlled variable within predetermined bounds around a reference value.

The hysteresis regulator serves as a basic current controller by directly controlling the on/off states of switches based on the current error. The operation principle of a hysteresis controller is as follows:

In a hysteresis regulator, as depicted in Figure 3.7, if the difference between the actual current and the desired command current exceeds a preset value known as the hysteresis band (denoted as h), the state of the switch is changed to reduce the error. Specifically, the switch state is altered based on whether the actual current is greater or lesser than the command current by the hysteresis band h. This is achieved by:

- Turning ON the lower switch to decrease the load current by generating a negative voltage.
- Turning ON the upper switch to increase the load current by generating a positive voltage.

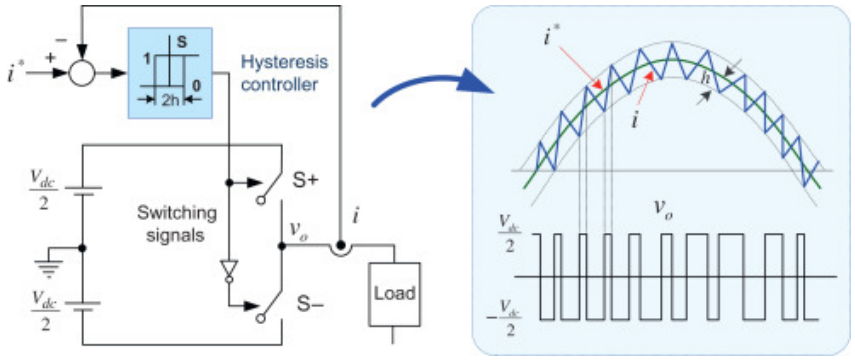

Figure 3.7: Operating principle of a hysteresis regulator

This approach effectively maintains the controlled variable within the desired bounds, preventing excessive deviations and ensuring stable operation of the system.

3.4.2 TAKAGI-SUGENO fuzzy logic speed-controller design

Fuzzy logic control is mostly used for high uncertainty non-linear systems. In this section, a Takagi-Sugeno fuzzy logic controller is designed for speed regulation and reference torque generation to improve the performance of a BLDC control scheme. The T-S method requires the least computation effort compared to other fuzzy inference methods . The zero-order TS-FLC is composed of three basic processes as shown in Figure 3.8 : fuzzification, rules base, and defuzzification

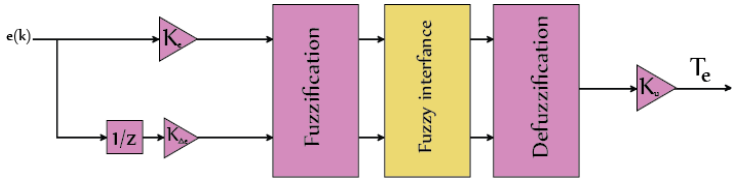

Figure 3.8: Block diagram of the proposed FLC

K_e, $K_{\Delta e}$, and K_u are the normalization factors.

The selection of input and output normalization factors is made based on the knowledge about the process. e(k)is the rotor speed tracking error. Figures 3.9 and 3.10 represent the proposed normalized input and output membership functions in terms of linguistic variables, NB (Negative Big), NM (Negative Medium),NS (Negative Small), ZE (Zero), PS (Positive Small), PM (Positive Medium), and PB (Positive Big). In the last step, a center weighted average algorithm is used in the defuzzification process.

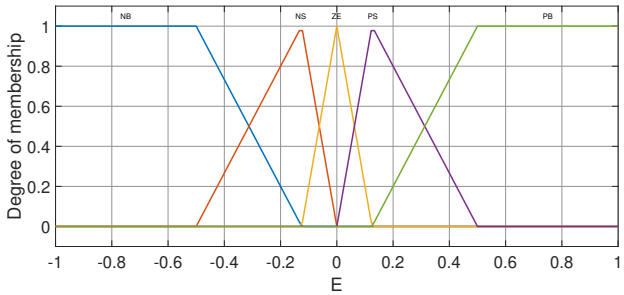

Figure 3.9: TS-FLC inputs membership functions

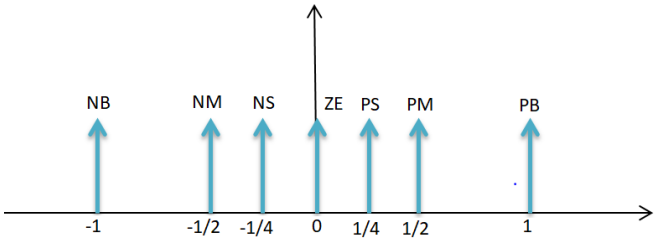

Figure 3.10: TS-FLC outputs membership functions

The fuzzy rules used in the proposed FLC can be represented in a symmetric form, as illustrated in Table 3.2

$\Delta e(K)$	$e(K)$				
	NB	NS	ZE	PS	PB
NB	NB	NB	NM	NS	ZE
NS	NB	NM	NS	ZE	PS
ZE	NM	NS	ZE	PS	PM
PS	NS	ZE	PS	PM	PB
PB	ZE	PS	PM	PB	PB

Table 3.2: Fuzzy logic speed control rules base

3.5 conclusion

This chapter provides a detailed overview of control approaches that facilitate intelligent power distribution in a hybrid system. By implementing these control algorithms, it becomes possible to effectively manage the power output from each source and ensure optimal control of the electric vehicle's traction system.

Chapter 4

Results and Discussion

4.1 Introduction

The performance of the system developed within this study has been thoroughly examined and validated through a series of comprehensive tests. These tests were designed to assess the system's capabilities and effectiveness in various operational scenarios. The following three distinct scenarios were carefully selected to cover different aspects of system performance:

Scenario 1: Constant Speed with Load Variation.

Scenario 2: Acceleration and Deceleration with Hybrid Energy Storage.

Scenario 3: Japanese Driving Cycle.

Through the analysis of these scenarios, the chapter aims to provide a comprehensive understanding of the system's performance. The results obtained will be used to assess control strategies, identify areas for improvement, and optimize system operation.

4.2 Simulation results

4.2.1 Scenario 1: Constant Speed with Load Variation

Figure 4.1 illustrates the performance of the hybrid electric vehicle (HEV) in terms of speed, and torque. When the load is added, we observed in Figure 4.1 (a) a slight decrease in the speed of the HEV. Conversely, when the load is removed, we noticed a slight increase in the speed of the HEV. With the reduced load, the motor requires less power to maintain the constant speed, allowing the vehicle to accelerate slightly. As shown

in Figure 4.1 (b) , when the load is added, we observed an increase in the motor's torque output. The additional load requires the motor to deliver more torque to overcome the increased resistance and maintain the constant speed. On the other hand, when the load is removed, we noticed a decrease in the motor's torque.

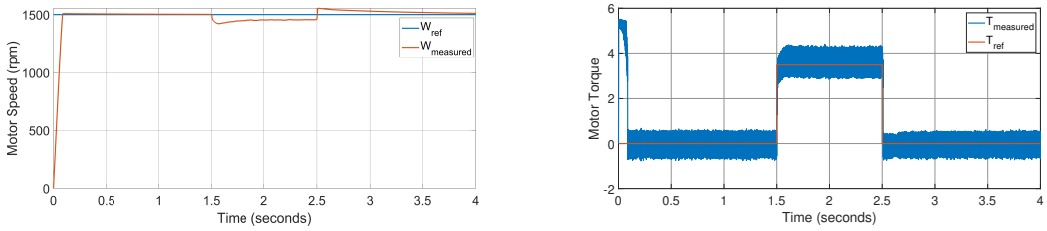

(a) HEV Speed (b) HEV Torque

Figure 4.1: HEV Performance: Speed, and Torque

In the constant speed scenario with load variation, we examined the performance of the battery and super-capacitor in terms of voltage, current, power, and state of charge (SOC). Figure 4.2 illustrates the behavior of the battery and super-capacitor voltages during load variation. When the load was applied, we observed a slight drop in the battery voltage Figure 4.2 (a) due to the increased power demand. While, as seen in Figure 4.2 (b) the super-capacitor voltage remains stable due to its ability to discharge quickly and provide instantaneous power support during load variations.

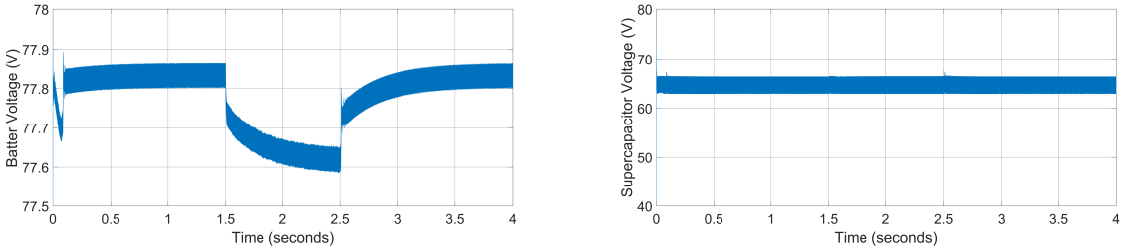

(a) Battery Voltage (b) Supercapacitor Voltage

Figure 4.2: Voltage Comparison: Battery and Supercapacitor

Moving on to the current analysis , Figure 4.3 presents the battery and super-capacitor currents during load variation. As the load was introduced, the battery current increased (Figure 4.3 (a)) to meet the higher power demand, ensuring continuous power supply. Conversely, when the load was removed, the battery current decreased accordingly. The super-capacitor current (Figure 4.3 (b))showcased its rapid response and high power capabilities, quickly adjusting to the load variations.

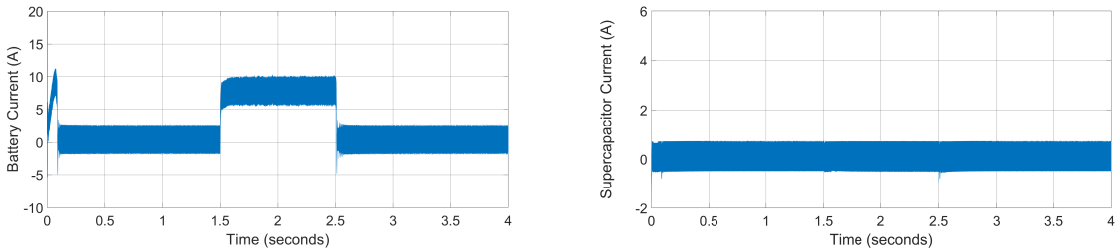

(a) Battery Current (b) Super-capacitor Current

Figure 4.3: Current Comparison: Battery and Super-capacitor

Figure 4.4 showcases the SOC levels of the battery and super-capacitor during load variation. When the load is applied, the battery's SOC gradually decreases as it supplies power to meet the increased demand. This reduction in SOC reflects the battery's discharge of stored energy to support the load. Conversely, when the load is removed, the battery's SOC experiences a slight decrease is observed as the power demand decreases. This indicates that the battery requires less energy to maintain the constant speed, allowing its SOC to increase slightly.On the other hand, the super-capacitor's SOC remains relatively unchanged during load variation since its high-power capability allows it to support the load without significant energy consumption.

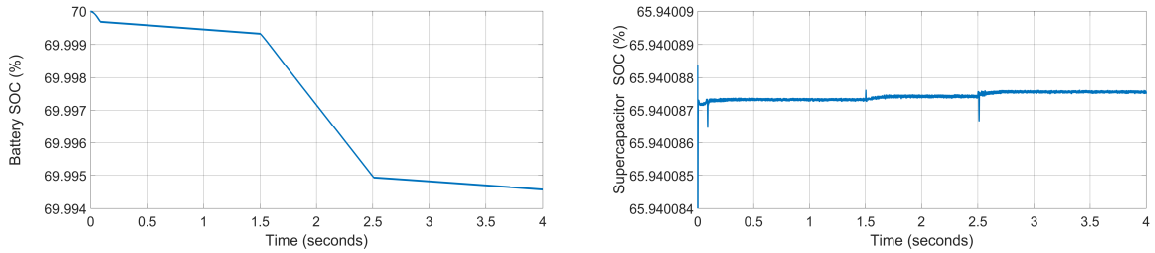

(a) Battery SOC (b) Super-capacitor SOC

Figure 4.4: SOC Comparison: Battery and Super-capacitor

Figure 4.5 (a) focuses on the battery power profile during different load conditions.

As the load is added to the HEV system, the battery power experiences a temporary increase. This is due to the higher power demand required to meet the additional load requirements. Conversely, when the load is removed, the battery power undergoes a decrease. With the reduced load, the power demand decreases, and the battery adjusts accordingly to supply the appropriate power.Since we are operating with a constant speed there is no power demand for the supercapacitor as shown in figure 4.5 (b).

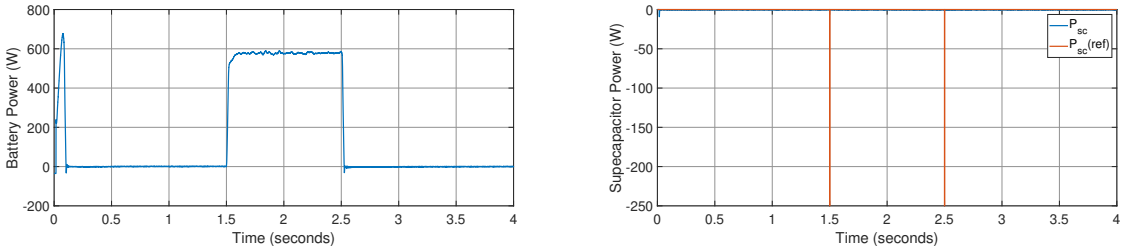

(a) Battery Power (b) Super-capacitor Power

Figure 4.5: Power Comparison: Battery and Super-capacitor

Figure 4.6 illustrates the performance of the hybrid electric vehicle (HEV) in terms of power.

From figure 4.6 (a) , it is evident that the power demand matches the sum of the battery and super-capacitor voltage. This indicates a balance between the power required by the load and the combined power output of the energy storage devices.Upon analyzing the figure, we can observe that whenever the power demand increases, the combined voltage of the battery and super-capacitor also rises in tandem. Similarly, when the power demand decreases, the voltage of the energy storage devices decreases accordingly.

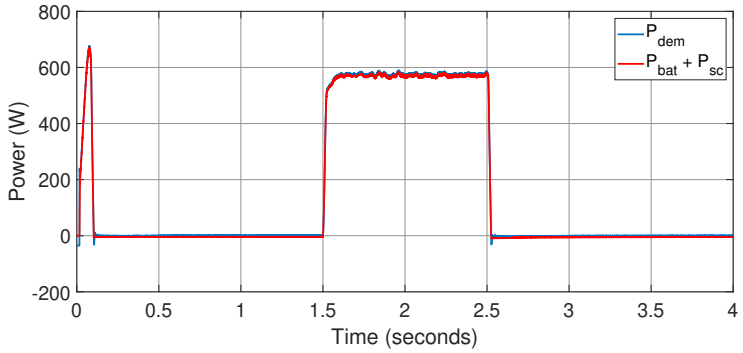

Figure 4.6: HEV performance : Power

During load application, we observed in Figure 4.7 a slight decrease in the DC bus voltage due to the increased power demand. As the load draws more current from the system, the voltage drops to accommodate the higher power transfer. Conversely, when the load is removed, the DC bus voltage shows a slight recovery as the power demand decreases. With reduced load, the voltage level increases to maintain the stability of the system.

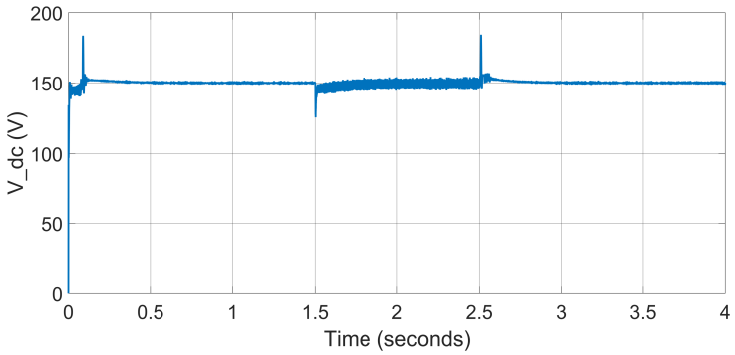

Figure 4.7: DC bus Voltage

By comparing the performance of the battery and supercapacitor, it becomes evident that the battery is responsible for delivering sustained power over longer durations, while the supercapacitor excels in providing immediate bursts of power. This combination of energy storage devices enables efficient power management in the constant speed scenario, ensuring reliable and stable operation of the system.

4.2.2 Scenario 2: Acceleration and Deceleration with Hybrid Energy Storage.

Scenario 2 aimed to assess the system's performance during acceleration and deceleration phases. The simulation focused on the utilization of the battery and supercapacitor (SC) components in a coordinated manner. During acceleration, the battery provided the necessary power, while during deceleration, the SC was charged through regenerative braking.

In the present work, a reference velocity profile is illustrated in figures 4.8 . The velocity curve is composed of three different modes: an acceleration mode between [1-2s], [5-6s], [9-10s]; a constant velocity mode between [2-3s], [6-7s], and [10-12s]; and a deceleration mode between [3-4s], [7-8s], and [12-13s]. The purpose of selecting this variable velocity profile is to assess the performance of the developed algorithms more effectively. We will specifically focus on the acceleration and deceleration modes.

The simulation results clearly show that the motor velocity perfectly tracks its reference, with almost zero overshoot and static error. The electromagnetic torque is represented by its stator current, Ia, which reflects the demanded load current by the traction part.

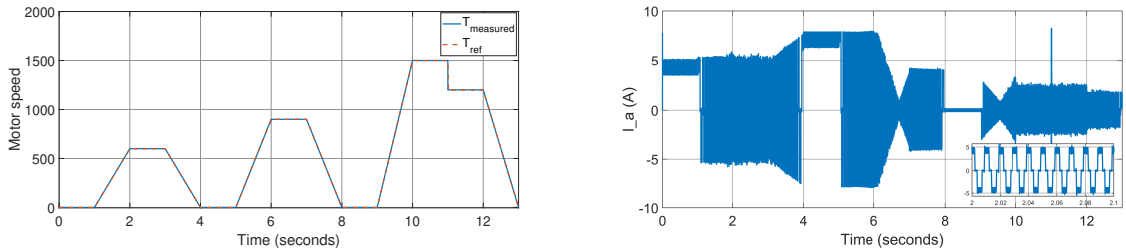

(a) Motor Speed (b) Motor current

Figure 4.8: Simulation results

In the acceleration mode, Figure 4.9 and Figure 4.10 illustrates the voltage and current profiles of the battery and super-capacitor. The battery voltage graph Figure 4.9 (a) demonstrates a slight decrease at the beginning of acceleration, while the battery current graph Figure 4.10 (a) exhibits a rapid rise. Similarly, the super-capacitor voltage graph Figure 4.9 (b) remains stable, and the super-capacitor current graph Figure 4.10 (b) shows a rapid increase.

During deceleration, the battery voltage graph shows a slight recovery, and the battery current graph changes direction to indicate regenerative braking. The super-capacitor voltage graph remains stable, and the super-capacitor current graph displays a reverse flow.

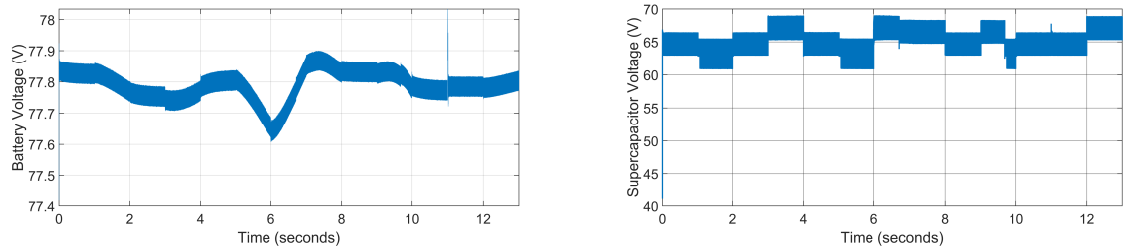

(a) Battery Voltage (b) Super-capacitor Voltage

Figure 4.9: Voltage Comparison: Battery and Super-capacitor

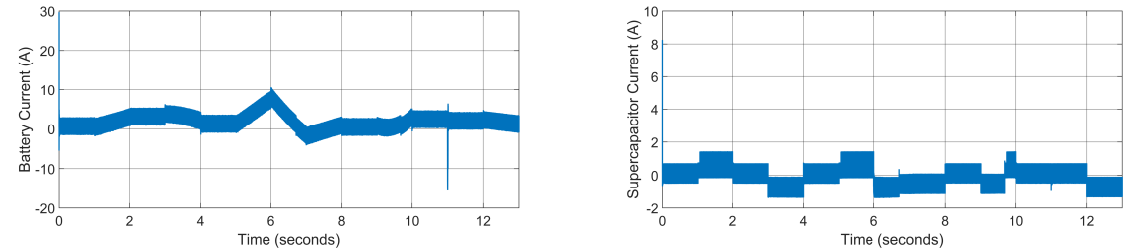

(a) Battery Current (b) Super-capacitor Current

Figure 4.10: Current Comparison: Battery and Super-capacitor

Figure 4.11 represents the State of Charge (SOC) of the battery and super-capacitor during acceleration and deceleration. In the acceleration mode, both the battery and super-capacitor exhibit a gradual decrease in SOC, indicating the discharge of stored energy to power the electric motor and meet the increased power demands. In the deceleration mode, the SOC of the battery shows a gradual decrease, indicating the discharge of stored energy as the regenerative braking process recovers and stores energy in the super-capacitor.

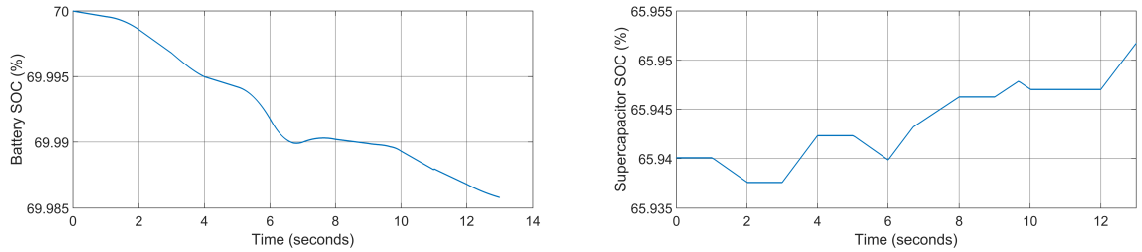

(a) Battery SOC

(b) Super-capacitor SOC

Figure 4.11: SOC Comparison: Battery and Super-capacitor

In Figure 4.12 (a) and (b), the power profiles of the battery and super-capacitor during acceleration and deceleration are depicted. During acceleration, the battery power gradually decreases as it discharges its stored energy to meet the increased power demands. Meanwhile, the super-capacitor power exhibits a corresponding increase, contributing to the overall power supply and ensuring rapid energy delivery for acceleration.

In the deceleration phase, where regenerative braking occurs exclusively with the super-capacitor, the power dynamics shift. The battery power output decreases significantly, as it is not actively involved in the regenerative process. On the other hand, the power profile of the super-capacitor shows a noticeable increase as it efficiently absorbs and stores the regenerated energy. This demonstrates the effective utilization of the super-capacitor for regenerative braking.

While in Figure 4.12 (c) , an important observation is made regarding the power balance in the system. The plot demonstrates that the sum of the battery power and super-capacitor power closely matches the power demand during both acceleration and deceleration. This alignment indicates that the combined power output of the battery and super-capacitor effectively meets the required power for the traction system.

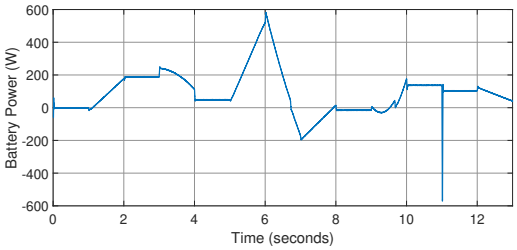

(a) Battery Power

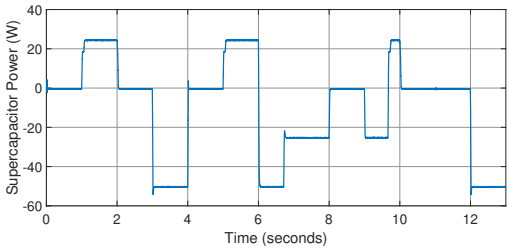

(b) Super-capacitor Power

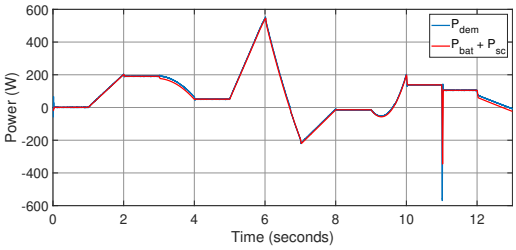

(c) HEV Power

Figure 4.12: Power Comparison: Battery and Super-capacitor

In Figure 4.13, the behavior of the DC bus voltage is presented. The plot illustrates that the DC bus voltage closely tracks its reference value of 150 V throughout the simulation. This indicates that the control system effectively regulates and maintains the DC bus voltage at the desired level.

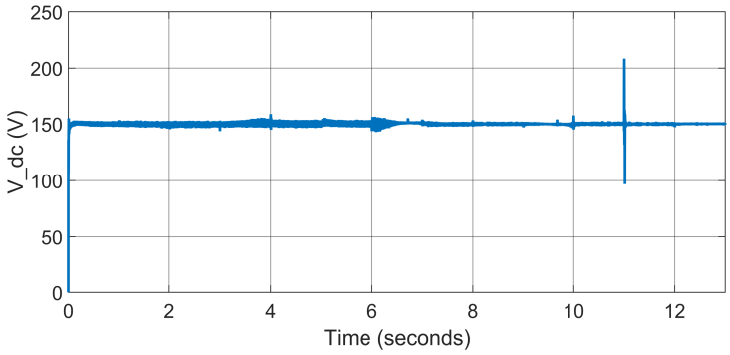

Figure 4.13: DC bus Voltage

In conclusion, the scenario of acceleration and deceleration with regenerative braking solely relying on the super-capacitor demonstrates the effective utilization of energy storage components in the hybrid electric vehicle system.

4.2.3 Scenario 3 : Japanese Driving Cycle.

The system's performance was tested using the Japanese driving cycle, representing real-world driving conditions. By simulating the specific speed and load profiles of the cycle described in figure 4.14 , the chapter evaluated the system's overall performances.

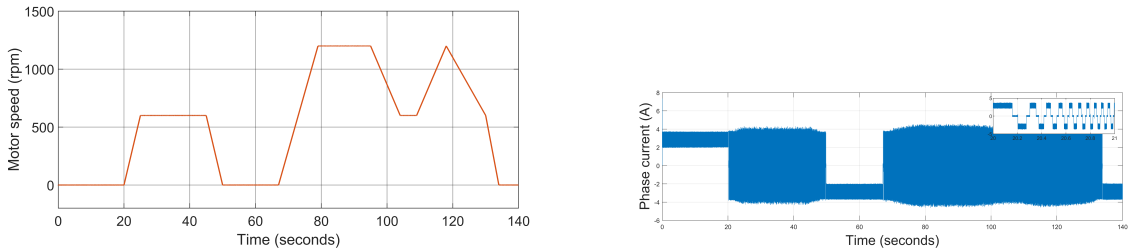

(a) Motor speed (b) Motor current

Figure 4.14: HEV performance

The simulation results for the Japanese driving cycle shown in Figure 4.15 and 4.16 demonstrate the voltage and current behavior of the battery and super-capacitor in various driving scenarios. During acceleration, the battery voltage decreases while the super-capacitor voltage remains stable. In deceleration, the battery voltage increases due to regenerative braking, while the super-capacitor voltage slightly decreases as it absorbs the regenerated energy.

During constant speed driving, both the battery and super-capacitor voltages remain steady, indicating a balanced power supply. It is important to note that regenerative braking is only applied to the super-capacitor, enabling efficient energy recovery.

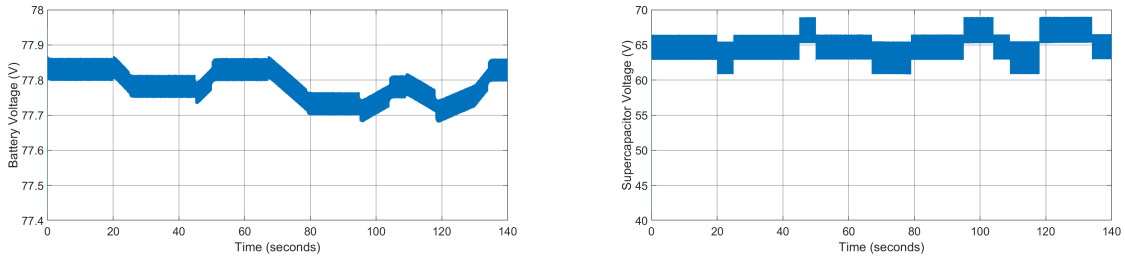

(a) Battery Voltage (b) Super-capacitor Voltage

Figure 4.15: Voltage Comparison: Battery and Super-capacitor

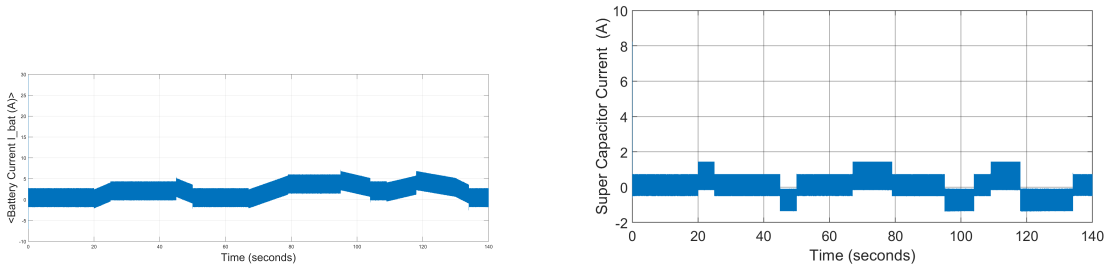

(a) Battery Current (b) Super-capacitor Current

Figure 4.16: Current Comparison: Battery and Super-capacitor

Figures 4.17 shows that the state of charge (SOC) of the battery and super-capacitor exhibits different behavior. During acceleration, the battery's SOC gradually decreases as it provides power, while the super-capacitor's SOC remains relatively stable. In deceleration, regenerative braking is applied exclusively to the super-capacitor, leading to an increase in its SOC as it captures and stores regenerated energy. During constant speed driving, both the battery and super-capacitor SOCs remain constant, indicating a balanced power supply.

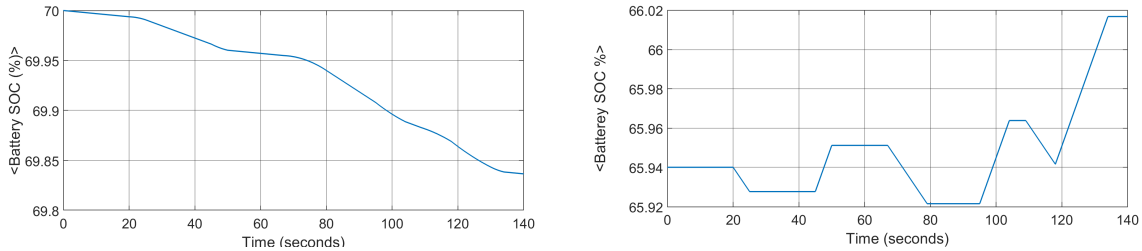

(a) Battery SOC (b) Super-capacitor SOC

Figure 4.17: SOC Comparison: Battery and Super-capacitor

The figures 4.18 demonstrates the power balance between the battery and super-capacitor in different driving modes . It demonstrates that the sum of power from both the battery and super-capacitor is equal to the power demand of the vehicle.

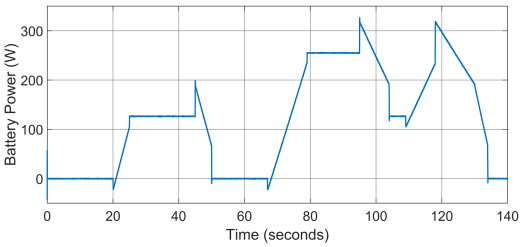

(a) Battery Power

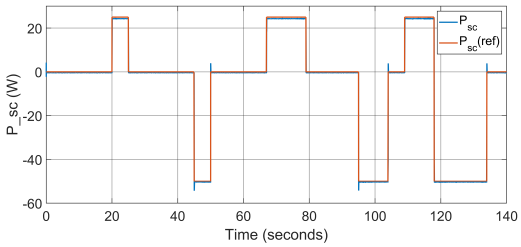

(b) Super-capacitor Power

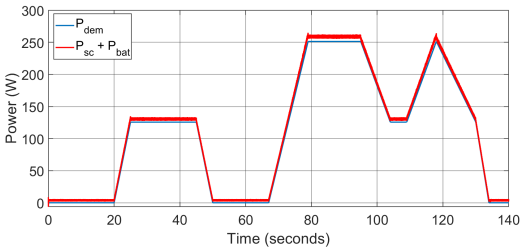

(c) HEV Power

Figure 4.18: Power Comparison: Battery and Super-capacitor and power demand

Figure 4.19 depicts the behavior of the DC bus voltage in the simulation. The plot clearly demonstrates that the DC bus voltage closely follows its reference value of 150 V throughout the entire simulation period.

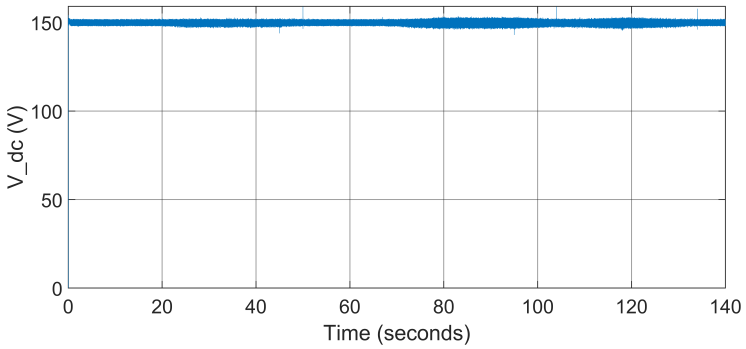

Figure 4.19: DC bus Voltage

4.3 Conclusion

The simulation results confirm that the developed system exhibits good performance in various operational scenarios, showcasing its ability to effectively manage power demand, utilize regenerative braking, and ensure a stable and efficient operation of the hybrid energy storage system.

General conclusion

This research work has focused on the energy management of a hybrid energy storage system in electric vehicles (EVs). The objective was to develop efficient and intelligent energy management strategies to optimize the performance and utilization of multiple energy sources in the hybrid system.

The simulation results have been carried out on Matlab/Simulink software, which proved that the fuzzy logic-based energy management system effectively regulates the power demand and its slop, maintains the state of charge of the supercapacitor, and ensures efficient power distribution based on the instantaneous power demands of the vehicle.

Moreover, the fuzzy logic control approach has proven to be robust and adaptable to varying driving conditions, allowing for smooth transitions between operating modes and optimal utilization of available energy sources. This has resulted in improved energy efficiency, extended range, and enhanced overall performance of the hybrid EV.

As a future work we propose :

- Real-time simulation and experimental implementation of the considered traction chain.
- The use of advanced learning based energy management techniques.

appendix

Design parameters	Value
Nominal voltage (V)	72
Rated capacity (Ah)	50
Initial state-of-charge (%)	70
Battery response time (s)	1

Table 4.1: Lithium-Ion battery parameters

Design parameters	Value
Rated capacitance (F)	165
Equivalent DC series resistance (Ohms)	2.9
Rated voltage (V)	96
Number of series capacitors	6
Number of parallel capacitors	1
Initial voltage (V)	65
Operating temperature (celsius)	25

Table 4.2: Super-Capacitor parameters

Design parameters	Value
Rated Torque Td	4.2 Nm
Rated Power Pd	1.5 kW
Rated Speed Nr	2880 rpm
Poles Nm	10
Phase Resistance Rph	0.7 Ohm
phase inductance Lph	4 mH
Torque constant Kt	0.7Nm/A
Moment of Inertia J	0.0028 kg/mˆ3

Table 4.3: BLDC Motor parameters

Bibliography

[1] EVBox, "Electric Cars: A Brief History," Available at: https://blog.evbox.com/electric-cars-history, accessed: June 18, 2023.

[2] J. Larminie and J. Lowry, *Electric Vehicle Technology Explained*. Chichester: John Wiley and Sons Ltd., 2003.

[3] C. P. Bottura and G. Barreto, *Electric Vehicles*. Campinas: UNICAMP, 1989.

[4] S. Mahapatra, T. Egel, R. Hassan, R. Shenoy, and M. Carone, "Model-based design for hybrid electric vehicle systems," The Mathworks Inc., Tech. Rep., January 2008.

[5] M. Ehsani, Y. Gao, and M. Miller, "Hybrid electric vehicles: Architecture and motor drives," *Proceedings of IEEE*, vol. 95, no. 4, pp. 719–728, April 2007.

[6] Futura Sciences, "Full Hybrid," https://www.futura-sciences.com/planete/definitions/developpement-durable-full-hybride-7284/, Accessed on June 20, 2023.

[7] x-engineer.org, "Mild Hybrid Electric Vehicle (MHEV) Components," https://x-engineer.org/mild-hybrid-electric-vehicle-mhev-components/, Accessed on June 20, 2023.

[8] A. Emadi, Y. J. Lee, and K. Rajashekara, "Power electronics and motor drives in electric, hybrid electric, and plug-in hybrid electric vehicles," *IEEE Transactions on Industrial Electronics*, vol. 55, no. 6, pp. 2237–2245, June 2008.

[9] "Driving plug-in hybrid electric vehicles: Reports from u.s. drivers of hevs converted to phevs, circa 2006-07," Unpublished report, 2006, accessed: June 18, 2023.

[10] EnergySage, "Pros and Cons of Electric Cars," Available at: https://www.energysage.com/electric-vehicles/101/pros-and-cons-electric-cars/, accessed: June 18, 2023.

[11] L. Ahmadi, A. Elkamel, and S. Abdul-wahab, "Multi-period optimization model for electricity generation planning considering plug-in hybrid electric vehicle penetration," *Energy Conversion and Management*, vol. 52, no. 1, pp. 448–456, 2011.

[12] Inside-EVs. (2017) EV Battery Makers 2016: Panasonic and BYD Combine to Hold Majority of Market. Accessed: February 21, 2021. [Online]. Available: https://insideevs.com/ev-battery-makers-2016-panasonic-and-byd-combine-to-hold-majority-of-market/

[13] S. Manzetti and F. Mariasiu, "Electric vehicle battery technologies: From present state to future systems," *Renewable and Sustainable Energy Reviews*, vol. 130, p. 109989, 2020. [Online]. Available: https://www.sciencedirect.com/science/article/pii/S1364032119309488

[14] T. Bartholome, K. Hankins, and N. Keller, "Lithium ion batteries: What are lithium ion batteries and how do they work?" *CHEM 362*, 2023, section 500.

[15] H. L. Ferreira, R. Garde, G. Fulli, W. Kling, and J. P. Lopes, "Characterisation of electrical energy storage technologies," *Energy*, vol. 53, pp. 288–298, 2013.

[16] U. A. Uparikar and H. V. Takpire, "Supercapacitor and battery power management in electric vehicle application," in *Conference Name*.

[17] A. G. Olabi, Q. Abbas, A. Al Makky, and M. A. Abdelkareem, "Supercapacitors as next generation energy storage devices: Properties and applications," *Energy*, vol. 248, p. 123617, June 2022.

[18] M. R. Ishaque, M. A. Khan, M. M. Afzal, A. Wadood, S.-R. Oh, M. Talha, and S.-B. Rhee, "Fuzzy logic-based duty cycle controller for the energy management system of hybrid electric vehicles with hybrid energy storage system," *Energies*, vol. 6, no. 1, pp. 246–266, 2013.

[19] A. Khaligh and Z. C. Li, "Battery, ultracapacitor, fuel cell, and hybrid energy storage systems for electric, hybrid electric, fuel cell, and plug-in hybrid electric vehicles-state

of the art," *IEEE Transactions on Vehicular Technology*, vol. 59, no. 6, pp. 2806–2814, July 2010.

[20] M. P. Neenu and S. Muthukumaran, "A battery with ultracapacitor hybrid energy storage system in electric vehicles," in *Proceedings of IEEE International Conference on Advances in Engineering, Science, and Management (ICAESM)*, March 2012, pp. 731–735.

[21] J. Cao and A. Emadi, "A new battery/ultra-capacitor hybrid energy storage system for electric, hybrid, and plug-in hybrid electric vehicles," in *Proceedings of IEEE Vehicle Power and Propulsion Conference*, September 2009, pp. 941–946.

[22] Z. Amjadi and S. Williamson, "Power-electronics-based solutions for plug-in hybrid electric vehicle energy storage and management systems," *IEEE Transactions on Industrial Electronics*, vol. 57, no. 2, pp. 608–616, February 2010.

[23] P. L. C. Q. X. L. Zhenpo Wang, Jin Zhang, "Driving cycle construction for electric vehicles based on markov chain and monte carlo method: A case study in beijing," *Proceedings of the 10th International Conference on Applied Energy (ICAE2018)*, 2018, peer-review under responsibility of the scientific committee of ICAE2018 – The 10th International Conference on Applied Energy.

[24] DieselNet, "Jp-10 mode driving cycle," Website, retrieved from https://dieselnet.com/standards/cycles/jp$_1$0*mode.php*.

[25] J. Shen, "Energy management of a battery-ultracapacitor hybrid energy storage system in electric vehicles," Ph.D. dissertation, University of Maryland, 2016.

[26] D. Rimpas, S. D. Kaminaris, I. Aldarraji, D. Piromalis, G. Vakas, P. G. Papageorgas, and G. Trakadas, "Energy management of storage systems on electric vehicles: A comprehensive review," in *Proceedings of the 2021 IEEE International Conference on Environment and Electrical Engineering and 2021 IEEE Industrial and Commercial Power Systems Europe (EEEIC / ICPS Europe)*, September 2021, pp. 814–819.

[27] F. Zhang, L. Wang, S. Coskun, H. Pang, Y. Cui, and J. Xi, "Energy management strategies for hybrid electric vehicles: Review, classification, comparison, and outlook," *Journal of Power Sources*, vol. 472, p. 228534, June 2020.

[28] M. SELLALI, "Commande d'un système multi-sources dédié au véhicule électrique," Ph.D. dissertation, Université Mohamed Khider–Biskra, 2020.

[29] V. Viswanatha and R. Venkata Siva Reddy, "A complete mathematical modeling, simulation and computational implementation of boost converter via matlab/simulink," *School of Electrical and Electronics Engineering, REVA University Bangalore, Karnataka, India*, May 2017.

[30] S. Mondal, A. Mitra, and M. Chattopadhyay, "Mathematical modeling and simulation of brushless dc motor with ideal back emf for a precision speed control," in *2015 IEEE International Conference on Electrical, Computer and Communication Technologies (ICECCT)*, 2015, pp. 1–5.

[31] M. Alzayed and H. Chaoui, "Efficient simplified current sensorless dynamic direct voltage mtpa of interior pmsm for electric vehicles operation," *IEEE Transactions on Vehicular Technology*, vol. 71, no. 12, p. 12701, December 2022.